

2010

INVESTIGATING THE IN VITRO EFFECTS OF MURINE CLCA3 ON HT29 MUCUS AND GOBLET CELL PHYSIOLOGY

Evangelos Giakoumatos
Western University

Follow this and additional works at: <https://ir.lib.uwo.ca/digitizedtheses>

Recommended Citation

Giakoumatos, Evangelos, "INVESTIGATING THE IN VITRO EFFECTS OF MURINE CLCA3 ON HT29 MUCUS AND GOBLET CELL PHYSIOLOGY" (2010). *Digitized Theses*. 4071.
<https://ir.lib.uwo.ca/digitizedtheses/4071>

This Thesis is brought to you for free and open access by the Digitized Special Collections at Scholarship@Western. It has been accepted for inclusion in Digitized Theses by an authorized administrator of Scholarship@Western. For more information, please contact wlsadmin@uwo.ca.

INVESTIGATING THE *IN VITRO* EFFECTS OF MURINE CLCA3 ON HT29 MUCUS AND GOBLET CELL PHYSIOLOGY

(Spine title: The Effects of mCLCA3 on HT29 Mucus and Goblet Cells)
(Format: Monograph)

by

Evangelos Giakoumatos
B.M.Sc. (Honors Specialization in Biochemistry)

Department of Biochemistry

Submitted in partial fulfillment
of the requirements for the degree of Master of Science

School of Graduate and Postdoctoral Studies
The University of Western Ontario
London, Ontario, Canada
August 2010

© Evangelos Giakoumatos 2010

THE UNIVERSITY OF WESTERN ONTARIO
SCHOOL OF GRADUATE AND POSTDOCTORAL STUDIES

CERTIFICATE OF EXAMINATION

Supervisor

Dr. Richard Rozmahel

Supervisory Committee

Dr. Gilles Lajoie

Dr. Harvey Goldberg

Examination Board

Dr. Gilles Lajoie

Dr. Susan Meakin

Dr. Robert Cumming

The thesis by

Evangelos Giakoumatos

entitled:

**Investigating the *in vitro* effects of murine CLCA3 on HT29 mucus and goblet cell
physiology**

is accepted in partial fulfillment of the
requirements for the degree of Master of Science

Date _____

Chair of Examination Board

ABSTRACT

The murine orthologue of the human calcium-activated chloride channel-1 protein (hCLCA1), mCLCA3, has been linked to regulating mucous properties due to its intimate association with mucin granule membranes of goblet cells. In particular, induced mCLCA3 expression via transgene introduction has been previously shown to significantly improve the intestinal Cystic Fibrosis (CF) phenotype in cystic fibrosis transmembrane conductance regulator- (Cfr) deficient mice, confirming its role as a modifier gene of CF. The specific biological or pathological function of the various CLCA members is unknown and their predicted role as ion channels has been disputed. The aim of this study was to investigate the effects of introducing and overexpressing the mCLCA3 gene on mucin synthesis, mucus composition and goblet cell development in the human colonic epithelial HT29 cell line. Results showed that expression of mCLCA3 significantly reduced gene expression of the mucin proteins, MUC1. Since MUC1 is expressed in all secretory epithelial cells, this indicates a potential role for the modulation of mucus composition by mCLCA3. Analysis of goblet cell morphometry by histological staining showed that almost two thirds of goblet cell populations contained mucus in HT29 cultures transfected with mCLCA3. This was a significant increase when compared to control HT29 treatments and closely resembled the goblet cell population of untreated HT29 cells. This demonstrates that mCLCA3, and potentially hCLCA1, could have a regulatory role in goblet cell physiology by promoting mucus retention in HT29 cultures. Additional work is required to establish the mechanism of its action on goblet cell pathophysiology but mCLCA3, and hCLCA1, may be important therapeutic targets for mucous-based diseases.

KEYWORDS: Cystic fibrosis (CF), modifier gene, mCLCA3, hCLCA1, HT29, mucus, mucin, MUC1, MUC2, MUC3B, MUC5AC, MUC5B, trefoil factor 3 (TFF3), goblet cells

ACKNOWLEDGEMENTS

I would like to express my gratitude to my family, friends and colleagues for their support while completing my project. I would also like to thank my supervisor, Dr. Richard Rozmahel, for giving me the opportunity to undertake my M.Sc. project. He was able to provide insight, encouragement and guidance during my Master's candidacy.

I am thankful to my advisory committee members, Dr. Gilles Lajoie and Dr. Harvey Goldberg, for generously taking the time to attend meetings and for providing great advice and direction in the completion of my project. I am greatly indebted to Dr. Goldberg for taking the time to review my thesis and providing excellent feedback. I would also like to thank Dr. Jim Koropatnick and Dr. Joe Mymryk for kindly providing the HT29 and Cos-7 cell lines along with other materials used in this work.

I would like to thank everyone from the Rozmahel lab for their assistance in the lab. I would like to extend my appreciation and gratitude to Mary Keet, who was able to offer technical advice throughout this study. I would also like to thank Dr. Zareen Amtul and Lynn Wang for their technical support. I am very thankful to my friends and colleagues; Wei Tang, Rudha Al-Rohani and Gillian Mount, who were always willing and able to discuss any ideas or difficulties we had with our studies and course-work.

TABLE OF CONTENTS

CERTIFICATE OF EXAMINATION	ii
ABSTRACT.....	iii
KEYWORDS	iv
ACKNOWLEDGMENTS	v
TABLE OF CONTENTS.....	vi
LIST OF TABLES	viii
LIST OF FIGURES	ix
ABBREVIATIONS	x
I. INTRODUCTION	1
I. A. CFTR and the link to CF	1
I. A. i. Mutations of CFTR	3
I. A. ii. Clinical presentations of CF	4
I. B. Modifier genes and CF	5
I. B. i. Genetic modifiers and CF mouse models.....	6
I. B. ii. Modifiers in CF patients.....	7
I. C. mCLCA3.....	8
I. C. i. CLCA family	8
I. C. ii. mCLCA3, expression profile and structure.....	9
I. C. iii. Overexpression of mCLCA3.....	12
I. D. Mucus	15
I. D. i. Mucins	18
I. D. ii. Trefoil Factors	23
I. E. Thesis Introduction	26
II. MATERIALS AND METHODS	28
II. A. HT29 cell culture and butyrate treatment	28
II. A. i. Cell culture media, passage, cryopreservation and revival.....	28
II. A. ii. Sodium butyrate treatment.....	30
II. B. mCLCA3 plasmid construction and transfection.....	31
II. B. i. Construction of pBS KS+ mCLCA3 plasmid	31
II. B. ii. Construction of pDream2.1-mCLCA3 plasmid.....	35
II. B. iii. Transfection of HT29 cultures using pDream2.1-mCLCA3 plasmid.....	36
II. C. mCLCA3 RNA expression.....	40
II. C. i. Reverse transcription PCR	41
II. C. ii. Quantitative real-time PCR.....	41
II. D. mCLCA3 protein expression	43
II. D. i. Total protein collection and quantitation	43

II. D. ii. mCLCA3 protein detection.....	44
II. D. iii. MUC3B protein detection.....	45
II. D. iv. β -actin normalization and densitometry quantitation	45
II. D. v. Protein alignment using Blast-P search tool	46
II. E. Histology	46
II. E. i. Cell culture on coverslips	46
II. E. ii. Alcian blue and nuclear fast red preparation.....	47
II. E. iii. Fixing and staining of cells	47
II. E. iv. Cell counts of stained cultures.....	48
II. F. Statistical analysis	48
III. RESULTS.....	49
III. A. Generation of differentiated HT29 cell lines (HT29-d)	49
III. B. Generation of stable HT29-CLCA3 cell lines	51
III. C. Generation of transient HT29-CLCA3 cell lines	53
III. C. i. Primer optimization and dissociation curves for qPCR analysis.....	53
III. C. ii. mCLCA3 detection in transient cell cultures by RT-PCR and qPCR	54
III. C. iii. mRNA analysis of the mucin family of genes and trefoil factor type 3	57
III. C. iv. Protein analysis of mCLCA3 and MUC3B	59
III. C. v. BLAST analysis	62
III. C. vi. Histological staining of cell cultures and goblet cell counts.....	64
IV. DISCUSSION.....	69
IV. A. Generation of chemically differentiated HT29 cells	70
IV. B. Stable expression of mCLCA3 in HT29 cultures	72
IV. C. Transient expression of mCLCA3 in HT29 cultures	73
IV. C. i. Effect of transient mCLCA3 expression on MUC and TFF3 transcripts ..	75
IV. C. ii. Effect of transient mCLCA3 expression on MUC3B protein	77
IV. C. iii. Effect of transient mCLCA3 expression on goblet cell morphometry.....	78
IV. D. Summary	82
V. FUTURE DIRECTIONS.....	84
VI. REFERENCES	85
CURRICULUM VITAE.....	94

LIST OF TABLES

Table 1.1. Expression profile of MUC genes and structure type of mucin proteins.....	19
Table 1.2. Expression profile of TFFs	23
Table 2.1. Oligonucleotide primers used for PCR experiments and DNA sequencing...	38
Table 2.2. Primer concentrations used for Real-Time PCR analysis	42
Table 3.1. Relative MUC and TFF3 gene expression in untreated and treated HT29 cultures	57
Table 3.2. Goblet cell counts in untreated and treated HT29 cell cultures	65

LIST OF FIGURES

Figure 1.1.	Topology of the translated CFTR protein	2
Figure 1.2.	Structural prediction for mCLCA3.....	11
Figure 1.3.	Proposed mechanism of goblet cell metaplasia in the lung via mCLCA3 expression	14
Figure 1.4.	General architecture of a goblet cell.....	16
Figure 1.5.	Predicted structures of gel-forming and membrane-bound mucins.....	21
Figure 1.6.	Amino acid sequence of TFF3.....	24
Figure 2.1.	pBS-mCLCA3 plasmid constructs	37
Figure 2.2.	pDream2.1-MCS vector map and pDream2.1-mCLCA3 plasmid construct	39
Figure 3.1.	Histological stain of HT29 vs HT29-d cell cultures and goblet cell population analysis	50
Figure 3.2.	RT-PCR of stable transfected HT29-CLCA3 and HT29-MCS cell lines ...	52
Figure 3.3.	Dissociation curves and amplification plots for mCLCA3 primer set and HT29 sample.....	55
Figure 3.4.	mCLCA3 messenger RNA analysis of transiently transfected HT29 cell cultures.....	56
Figure 3.5.	qPCR results of relative MUC and TFF3 mRNA levels	58
Figure 3.6.	mCLCA3 Western blot and densitometry results.....	60
Figure 3.7.	MUC3B Western blot and densitometry results.....	61
Figure 3.8.	Sequence alignment of mCLCA3 antibody to human CLCA1 and -4.....	63
Figure 3.9.	Histological stain of untreated HT29 and treated HT29 cell cultures	66
Figure 3.10.	Goblet cell population analysis of cell culture stains	68

ABBREVIATIONS

ADP	adenosine diphosphate
ATP	adenosine triphosphate
B6	C57Bl/6 mouse
β -ME	beta-mercaptoethanol
BSA	bovine serum albumin
cAMP	cyclic adenosine monophosphate
cDNA	complementary DNA
CF	cystic fibrosis
CFTR	cystic fibrosis transmembrane conductance regulator
Cftr	murine cystic fibrosis transmembrane conductance regulator
Cftr ^{tm1HSC}	targeted mutation of exon 1 in murine Cftr
Cftr ^{tm1UNC}	targeted mutation of exon 10 in murine Cftr
CIAP	calf intestinal alkaline phosphatase
CK	cysteine knot-like domain
CLCA	chloride channel, calcium-activated
Cos-7	African green monkey kidney cell line
DMSO	dimethyl sulphoxide
EDTA	ethylene-diamine-tetraacetate
EGF	epidermal growth factor
EGF-R	epidermal growth factor receptor
ER	endoplasmic reticulum
ERK	extracellular-signal-regulated kinase
F ₁	first generation hybrid
FBS	fetal bovine serum
FnIII	fibronectin type III
GI	gastrointestinal
Hdj-2	heat shock protein J2
HGF	hepatocyte growth factor
HRP	horseradish peroxidase
Hsc70	heat shock cognate protein 70
Hsp90	heat shock protein 90
HT29	human colonic adenocarcinoma cell line
HT29-CaP	HT29 cultures treated with calcium phosphate transfection mix
HT29-CLCA3	HT29 cultures stably transfected with pDream2.1-mCLCA3
HT29-d	HT29 cultures chemically differentiated with NaBt
HT29-MCS	HT29 cultures stably transfected with pDream2.1-MCS
HT29trCLCA3	HT29 cultures transiently transfected with pDream2.1-mCLCA3
HT29trMCS	HT29 cultures transiently transfected with pDream2.1-MCS

IL	interleukin
ITF	intestinal trefoil factor (a.k.a. trefoil factor type 3)
LB	Luria broth
MARCKS	myristoylated alanine-rich C kinase substrate
MEK	mitogen-activated protein kinase kinase
MIDAS	metal ion-dependent adhesion site
mRNA	messenger RNA
MSD	membrane spanning domain
MUC	mucin gene(s)/protein(s)
NaBt	sodium butyrate
NBD	nucleotide binding domain
pBS KS+	Bluescript KS+ plasmid
P _i	inorganic phosphate
PI3K	phosphatidylinositol 3-kinase
PKA	protein kinase A
PKC	protein kinase C
PKG	protein kinase G
PVDF	polyvinylidene fluoride
qPCR	quantitative real-time PCR
RD	regulatory domain
RER	rough endoplasmic reticulum
RT	reverse transcriptase, (+) treated, (-) untreated
RT-PCR	reverse transcript polymerase chain reaction
SDS	sodium dodecyl sulphate
SEA	sea urchin sperm protein, enterokinase and agrin modules
SEM	standard error of the mean
STAT	signal transducers and activator of transcription
TFF	trefoil factor
TGF- α	transforming growth factor alpha
TGF- β	transforming growth factor beta
Th2	type-2 T helper cells
TM	transmembrane domain
UNC·B6	C57Bl/6 mouse carrying the Cfr ^{tm1UNC} mutation
UV	ultraviolet
VNTR	variable number of tandem repeats
VWA	von Willebrand factor type A
WT	wild-type

I. Introduction:

I. A. CFTR and the link to CF

Cystic fibrosis is an autosomal recessive genetic disorder caused by mutations in the cystic fibrosis transmembrane conductance regulator (CFTR) gene. The full-length CFTR protein is expressed primarily in the apical membrane of epithelial cells [1, 2] and its structure consists of two membrane spanning domains (MSD), two nucleotide binding domains (NBD) and a central regulatory domain (RD) organized in a symmetrical fashion (MSD1- NBD1- RD- NBD2- MSD2) (Figure 1.1) [3, 4]. CFTR is a member of the ATP-binding cassette family of transporter proteins and acts as a cAMP regulated chloride channel considered to be essential in maintaining ion and fluid homeostasis on epithelial surfaces [5-8]. Each half of the MSD in CFTR forms a pore on the ion channel, although the exact configuration of each domain remains unclear [9, 10]. PKA phosphorylation of the regulatory domain triggers conformational movements between the two NBDs and leads to rearrangements of the subunits within the MSDs; this causes a shift between the open and closed state of the ion pore, reviewed by Rowntree *et al.* in [8]. Chloride conductance through CFTR into the lumen induces paracellular fluid secretion, where water molecules move through gap junctions of the epithelial layer and into the lumen, leading to proper hydration of the mucosal layer. Dysfunctional CFTR causes salt imbalance on the epithelium and leads to thick viscous mucus in CF patients.

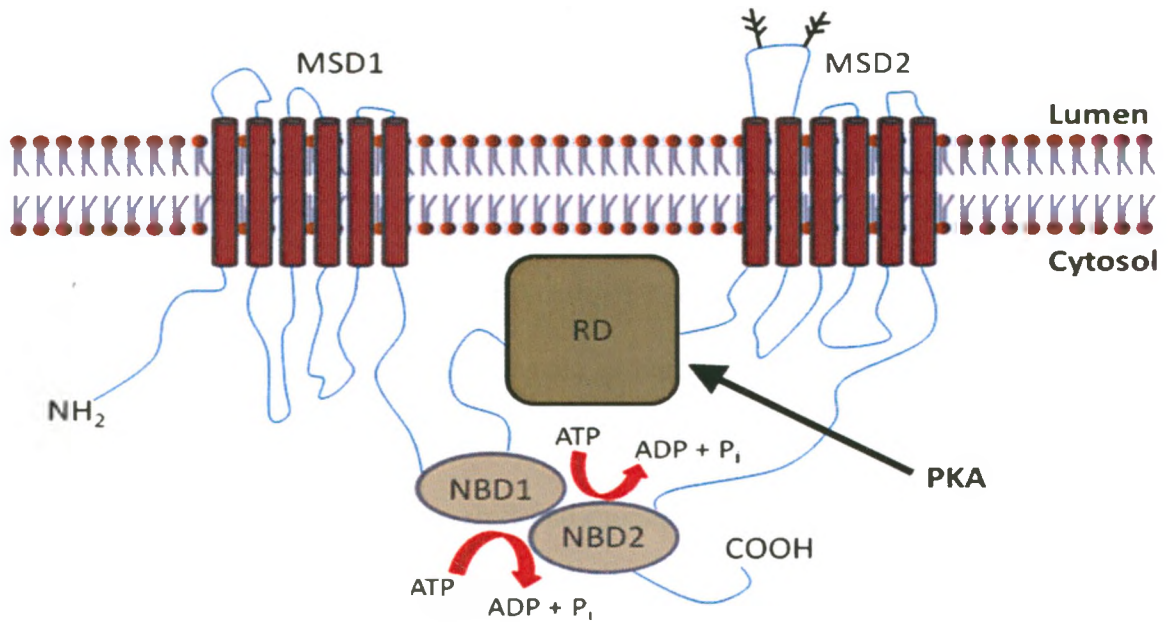


Figure 1.1. Topology of the translated CFTR protein. Localization of CFTR domains are shown relative to the cell's apical membrane. Phosphorylation of the regulatory domain (RD) by PKA changes the conformation of both nucleotide binding domains (NBD1, -2) and rearranges the subunits of each membrane spanning domain (MSD1, -2). This shifts the ion pore between the open and closed state. NBD1 and -2 can interact, forming a dimer-complex responsible for ATP hydrolysis. Glycosylation of CFTR on the fourth extracellular loop, on MSD2, enhances folding and stability of the membrane protein [11]. Figure adapted from [3].

I. A. i. Mutations of CFTR

There are currently over 1700 mutations of the CFTR gene listed in the CFTR mutation database (<http://www.genet.sickkids.on.ca/cftr>) with the $\Delta F508$ mutation being the most prevalent, accounting for 70% of CF chromosomes in most Caucasian populations [4, 12, 13]. This mutation causes a 3 bp deletion within exon 10 of the CFTR gene, leading to a loss of the amino acid phenylalanine at residue 508 [12] in NBD1 of the CFTR protein.

Mutations of CFTR can disrupt function by several mechanisms depending on the type of mutation and location. Mutations are grouped into six classifications (Classes I-VI) based on known or predicted protein products, reviewed by Zielenski in [3]. Class I mutations include nonsense, frame shift and missense mutations. These mutations cause defective and unstable protein to be synthesized and are rapidly degraded [3, 8]. Class II mutations, of which the $\Delta F508$ mutation is classified, lead to incorrect processing and transport of the protein. These proteins are not only misfolded but they also fail to reach the apical membrane [3], which is the surface of the cell membrane in polarized cells contacting the lumen. Class III mutations influence the regulatory domain of CFTR leading to non-functioning protein at the apical membrane [3]. Class IV mutations yield normal amounts of CFTR protein at the apical membrane, but with decreased ion conductance [8]. Class V mutations lead to decreased expression/production of CFTR protein and Class VI mutations result in CFTR protein with decreased stability [3]. Ultimately, these mutations lead to dysfunctional CFTR protein and/or abnormal trafficking of the protein to the apical membrane, causing CF.

CFTR translation is highly regulated, with systems in place that act as quality controls during synthesis, assembly and export. Approximately one third of CFTR nascent chains are processed into mature protein [14], while the remainder is degraded by proteosomes following ubiquitination [15, 16]. Proper folding and assembly of the large CFTR domains is regulated through interactions with chaperones and co-chaperones such as; Hsc70 [17], Hsp90 [18], calnexin [19], Hdj-2 [20] among others (reviewed by Riordan in [21]). The various classes of CFTR mutations that contribute to the CF phenotype either trigger degradation or, despite this complex regulation of synthesis, reach the apical membrane of epithelial cells with decreased function.

I. A. ii. Clinical presentations of CF

CF affects the fluid secreting epithelial cells of several organs. The severity of CF is not only variable from patient to patient, but there is also variability in the affected organs among patients [22]. Affected organs include the liver [23], pancreas [22], sweat glands [22] and genitourinary tract [24, 25]. Other organs seriously affected in CF patients are the respiratory system and the gastrointestinal (GI) tract, described in more detail below. The common defect of all CF patients is thick, dehydrated mucus (sputum) which results in a lack of mucus clearance and leads to obstruction of the airways, GI tract and other ducts.

CF patients are at high risk of bacterial infection in the lung by *Haemophilus influenza* [26], *Staphylococcus aureus* [26], *Pseudomonas aeruginosa* [27], *Streptococcus pneumoniae* [28] and *Mycoplasma pneumoniae* [29]. Lung disease is the primary cause of ailment and death in CF patients and is very difficult to treat. Normally

mucus acts to trap bacteria and is followed by mucus clearance, but lack of mucociliary clearance in CF leads to pulmonary infection. Inflammation, goblet cell hyperplasia and increased mucus secretions further complicate the CF lung disease and cause bronchiectasis [26], where bronchi become further inflamed, dilated and susceptible to collapse. This can lead to severe respiratory failure and death [26]. Current treatments include: helping clear the mucus with physiotherapy; administration of hypertonic saline to help hydrate the mucus; using a recombinant human DNase that helps reduce viscosity through degradation of polymerized DNA present in mucus; and administration of anti-inflammatory and/or antibiotic medication, reviewed by Kreindler in [30].

CF patients can also be affected by enteropathy, causing lesions of the intestinal lumen. The altered intestinal mucosa of CF patients has been suggested to cause lesions specifically in sites described to normally have high expression of CFTR [31], but the source of mucous-mediated lesions in CF is still not well understood. The dehydration of the secreted mucus in the intestinal lumen can also cause distal intestinal obstruction. Partial or complete bowel obstruction occurs because of abnormally viscous mucofaeculent material in the ileum and caecum, which should normally be in liquid-phase [32-34]. These factors cause poor intestinal absorption in approximately 90% of patients and to avoid malnutrition, patients are placed on high-fat high-energy diets [35].

I.B. Modifier genes and CF

The variation of CF severity is not solely due to the different classes of CFTR mutations; variation of severity has also been attributed to secondary genetic factors, also known as modifier genes. The differential expression of modifier genes from patient to

patient is thought to ameliorate the side effects of dysfunctional CFTR protein. CF mouse models have been used to study the various mutations involved in CF and have helped to elucidate potential modifier genes.

I. B. i. Genetic modifiers and CF mouse models

CF mice have been developed using targeted mutations of the murine *Cftr* gene. In a study conducted by Rozmahel and colleagues, a CF mouse line was established with a targeted mutation disrupting exon 1 of *Cftr* and was designated *Cftr*^{tm1HSC} [36]. The founder 129/sv mouse carrying the *Cftr*^{tm1HSC} mutation was bred with a CD1 female, the hybrid F₁ progeny heterozygous for the *Cftr* (+/*Cftr*^{tm1HSC}) were intercrossed to generate the homozygous (*Cftr*^{tm1HSC}/*Cftr*^{tm1HSC}) CF mice [36]. Most CF mice developed severe intestinal obstruction that lead to death within the first three weeks of life, but 30% survived beyond six weeks of age [36].

The 129/sv (+/*Cftr*^{tm1HSC}) mice were also crossed with C57Bl/6, BALB/C and DBA/2J strains and the F₁ heterozygotes were intercrossed to obtain CF mice of different inbred strains [36]. Results showed that genetic backgrounds among the inbred strains had significant effects on the survival of the CF mice [36]. A genome scan revealed a modifier locus, unlinked to the *Cftr* gene, on mouse chromosome 7 that can diminish the severity of the disease in (*Cftr*^{tm1HSC}/*Cftr*^{tm1HSC}) mice [36]. This locus was designated *Cfm1* and is syntenic to human chromosome 19 [36, 37], leading to the study of potential modifier genes of CF in humans.

I. B. ii. Modifiers in CF patients

Much like the variability seen among mice with different genetic backgrounds but carrying the same *Cftr*^{tm1HSC} mutation [36], variability of CF in humans also occurs among patients with the same CFTR mutations. The inconsistency of clinical presentation of CF patients strongly suggests that secondary genetic factors are influencing the CF phenotype. A potential modifier of meconium ileus, the obstruction of the ileum in CF newborns due to viscous mucus [38], was found on human chromosome 19q13 [37] and is syntenic to murine chromosome 7 [36, 37].

Secondary genetic factors in CF patients have been established through probable modifying effects on the severity of CF lung disease. These modifiers were initially studied due to their potential function in pathways directly related to airway inflammation, or because these genes play an important role in diseases similar to CF, such as asthma or chronic obstructive pulmonary disease [39]. To date, 13 modifier gene candidates of CF lung disease have been studied in two or more populations of CF patients, but analysis of these potential modifiers becomes difficult due to variable environmental factors and inconsistent effects of modifier gene polymorphisms among subsets of CF patients, reviewed by Collaco *et al.* in [39]. One example of a gene recently identified as a modifier of CF lung disease is interferon-related developmental regulator 1 (IFRD1), which is primarily expressed in neutrophils [40]. Mice deficient in *Ifrd1* showed delayed clearance of bacteria from the lungs but also had less neutrophilic inflammation [40]. This demonstrates the complexity of studying the effects of modifier genes as IFRD1 likely improves the clearance of bacteria, but it could exacerbate inflammation in the CF lung via neutrophil recruitment.

Continued study of modifier genes for CF may help to establish novel therapies and treatments for patients. The calcium-activated chloride channel (CLCA) family of genes, with a locus on human chromosome 1, have been linked to residual intestinal chloride ion currents [41] and were identified as potential modifiers of CF. A study by the Rozmahel lab, done in order to identify potential modifiers of CF, used microarray analysis (Affymetrix GenechipTM) to compare global gene expression in the lungs of C57Bl/6 -CF (*Cftr*^{im1UNC}/*Cftr*^{im1UNC}) (severe CF phenotype) and BALB/C -CF (*Cftr*^{im1UNC}/*Cftr*^{im1UNC}) (moderate CF phenotype) mice [42]. The gene encoding mCLCA3 was found to have significantly lower expression in C57Bl/6 -CF lungs but increased expression in BALB/C -CF lungs [42]. This was confirmed by RT-PCR and northern blots [42]. Other results showing differential expression of mCLCA3 in the intestine and lung of CF mice strengthen the argument that mCLCA3 is a potential modifier of CF [43].

I. C. mCLCA3

I. C. i. CLCA family

The first members of the calcium-activated chloride channel (CLCA) family were identified independently in two laboratories in 1991 [44, 45]. Bovine tracheal calcium-activated chloride channel [44] and bovine lung endothelial cell adhesion molecule-1 [45] were discovered by protein purification and later renamed bCLCA1 and bCLCA2, respectively. The two gene products were homologous and showed a calcium-dependent chloride conductance in secretory epithelial cells [46, 47]. Whole cell or single-channel patch clamp studies of CLCA transfected heterologous cell lines showed transmembrane

currents mediated by calcium ionophores [48-54]. These results agreed with the initial predictions of CLCA protein models as having several transmembrane domains and functioning as ion channels [55]. CLCA proteins were believed to augment CFTR's chloride ion conductance and therefore were primarily responsible for cellular chloride ion conductance in the absence of functional CFTR. As a result, these proteins were named chloride channels, calcium-activated. Since then, many additional CLCA gene homologues have been discovered in over thirty species, reviewed by Patel *et al.* in [56].

The human homologues of CLCA include hCLCA1 [53, 57], hCLCA2 [57, 58], hCLCA3 [58] and hCLCA4 [57]; these genes are localized on human chromosome 1, reviewed by Loewen *et al.* in [59]. In general, full-length CLCA proteins are ~100kDa when unprocessed but with glycosylation the mass ranges from ~110 - ~120kDa [56, 59]. CLCA proteins can then undergo additional processing through a cleavage step that yields ~85kDa N-terminal and ~35kDa C-terminal subunits [56], but processing and secretion of CLCA proteins can vary. The suggested function of CLCA proteins being calcium activated chloride channels has not been universally accepted as some members, like mCLCA3, have been shown to be soluble, secreted proteins [60].

I. C. ii. mCLCA3, expression profile and structure

The mCLCA3 gene (a.k.a. Gob-5), the murine orthologue to hCLCA1, was initially cloned from the mouse intestine [61]. mCLCA3 is located on mouse chromosome 3 [62] and is specifically expressed in mucin granules of epithelial goblet cells within the gastrointestinal tract, lung, trachea and uterus [63, 64]. The mCLCA3 gene is 28.2 kb long with 14 exons; the mRNA transcript is just over 2.9 kb long and

encodes a 913 amino acid protein. The holoprotein is 100 kDa but when glycosylated with mannose-rich oligosaccharides it has a mass of ~110 kDa product [63, 64]. Processing of this protein results in 75 kDa N-terminal and 35 kDa C-terminal peptides [60]. The soluble, secreted cleavage products of mCLCA3 have been shown to maintain association both inside and outside the cell [60].

Initially presumed to have five transmembrane domains (refuted by [60, 64]), there were serious discrepancies for the proposed models of CLCA proteins as transmembrane ion channels [56]. Figure 1.2 shows the suggested structural scheme of mCLCA3 based on structural prediction software. Following the initial peptide signalling sequence, there is an N-terminal cysteine-rich domain that is conserved among all members of the CLCA protein family [56]. The protein also has a von Willebrand factor type A (VWA) domain that spans residues 306 through 459 and a fibronectin type III (FnIII) domain from residues 748 through 870 [56]. VWA domains are involved in protein-protein interactions, usually by the coordination of a divalent cation interacting at the binding surfaces through metal ion-dependent adhesion sites (MIDAS) [65]. MIDAS motifs, located within the VWA domain, have a highly conserved set of five residues (DXSXS) and stabilize protein-protein interactions by chelating magnesium or calcium ions [56, 59]. VWA domains are often found in cell-adhesion and extracellular matrix proteins [66]. The FnIII domain is present within the C-terminal β -strand region of mCLCA3. These domains are usually involved in cell surface binding and are a part of extracellular domains of membrane-receptor proteins [67]. The current structural model of mCLCA3 suggests that it cannot act as an ion channel alone but most likely acts as a signalling factor interacting with proteins such as secondary chloride ion channels.

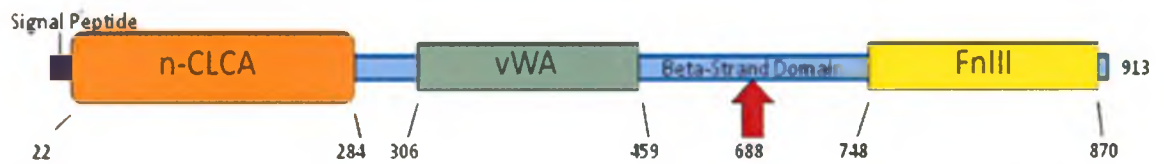


Figure 1.2. Structural prediction for mCLCA3. Schematic of domain structure for mCLCA3 protein showing the signalling peptide, the conserved N-terminal CLCA domain (n-CLCA, residues 22 through 284), the von Willebrand factor type A domain (VWA, residues 306 through 459) and fibronectin type III domain (FnIII, residues 748 through 870). The red arrow indicates the putative cleavage site at residue 688 located in the protein's beta-sheet structure. Figure adapted from [56, 64].

I. C. iii. Overexpression of mCLCA3

The exact function(s) of the CLCA family of proteins have yet to be established. The specific localization of mCLCA3 in mucin granules strongly suggests a role in goblet cell proliferation, discussed in more detail below. mCLCA3's intimate association with mucin granules also suggests a role in the synthesis, secretion or processing of mucus/mucin proteins. Overexpression of mCLCA3 in the human mucoepidermoid cell line NCI-H292 induced mucus production, specifically MUC5AC but the mechanism of action remains unclear [68].

The biological role of mCLCA3 has also been linked to airway diseases in mouse models but a Gob-5 (mCLCA3) knockout showed no clear intestinal phenotype [69], suggesting possible overlapping function by other CLCA family members or other modifier genes. This mouse also showed no requirement for mCLCA3 in order for the allergic asthma response with ovalbumin treatment [69]. In another study conducted using a mouse model of asthma, it was found that addition of adenoviral expressed mCLCA3 by injection into the trachea caused goblet cell metaplasia and airway hyper-responsiveness following ovalbumin treatment [68]. The same study used antisense mCLCA3 mRNA which caused suppression of airway hyper-reactivity and mucus production [68]. Other studies have shown that mice with asbestos-induced lung disease had an accumulation of mucus along with increased mCLCA3 protein levels [70], while mCLCA3 knockout mice that were induced to have pulmonary inflammation using ovalbumin had decreased goblet cell metaplasia and decreased mucus production [71]. These results support mCLCA3's role in goblet cell proliferation and increased mucus production in the lung.

In the congenic C57BL/6J mouse strain homozygous for the *Cfr*^{tm¹UNC} genetic knockout (UNC·B6 ^{-/-}), containing an engineered stop codon within exon 10 that mimics the Δ F508 mutation seen in human CF patients, mice develop severe lung and intestinal disease and this mouse line has become an important model for studying CF pathophysiology in both tissues [72]. Expression of mCLCA3 in UNC·B6 (^{-/-}) intestine is significantly lower than WT intestine [73]. Upregulation of mCLCA3 in the intestine of UNC·B6 (^{-/-}) mice caused amelioration of the CF phenotype and helped increase survival of *Cfr* deficient mice [73]. Although goblet cell hyperplasia and hypertrophy resulted from mCLCA3 overexpression, the intestinal lumen of the transgenic mice lacked the thick mucus seen in CF mice and instead resembled that of WT mice [73].

Studies on mCLCA3 certainly show augmentation of mCLCA3-mediated goblet cell proliferation and an increase in mucus production. The goblet cell hypertrophy observed in [73] suggests that mCLCA3 could potentially have an additional role in regulating intestinal mucus secretion. Figure 1.3 shows the suggested mechanism that could help to explain goblet cell metaplasia caused by mCLCA3 overexpression in the lung. In this model, interleukin (IL)-13 promotes mCLCA3 expression through the STAT6 signalling pathway [74]. The cleavage products of mCLCA3 are then thought to activate signalling molecules and induce mucin gene expression. Mucin gene overexpression is thought to contribute to goblet cell differentiation/metaplasia [56]. A transgenic mouse overexpressing IL-9 has also been shown to upregulate mCLCA3 and these mice develop an asthma-like phenotype [75]. Other Th2 cytokines, in addition to IL-13, like IL-4, have been shown to promote the expression of other mucins including

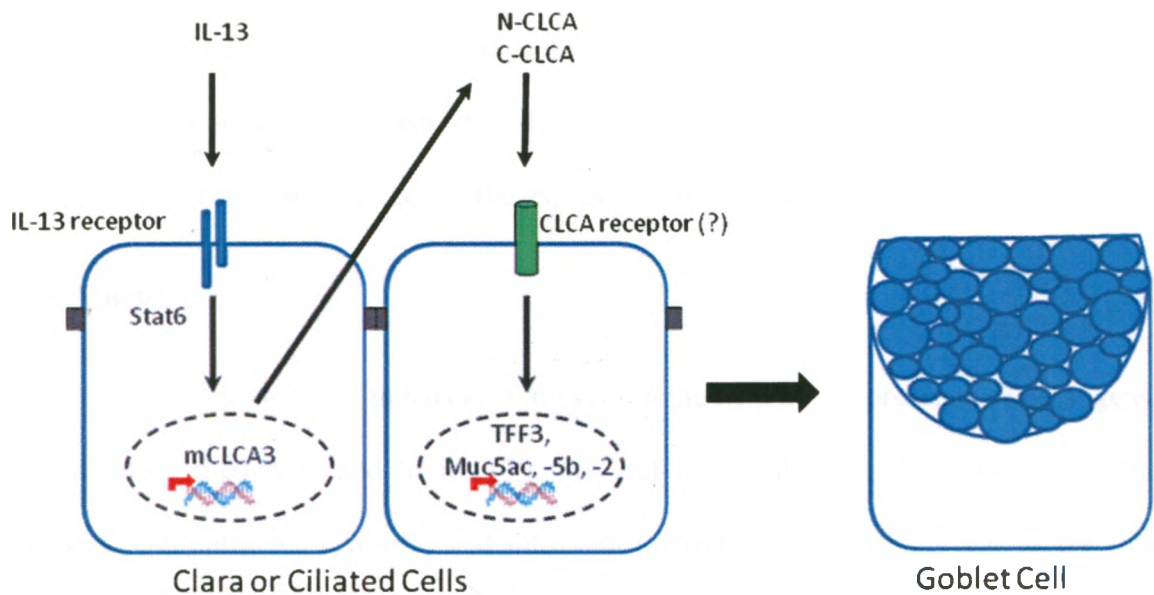


Figure 1.3. Proposed mechanism of goblet cell metaplasia in the lung via mCLCA3 expression. IL-13 has been shown to up-regulate mCLCA3 expression through STAT6 signalling [74]. The secreted CLCA peptides may then lead to activation of signalling molecules and cause mucin gene expression on neighbouring cells or the same cell, leading to goblet cell differentiation. The mechanism of this suggested signalling pathway has yet to be clarified and much work remains to decipher how mCLCA3 overexpression induces goblet cell metaplasia in the lung. Blue ovals represent mucus-filled mucin granules of the goblet cell, figure adapted from [56].

MUC5AC, MUC5B, MUC2 and the signalling trefoil factor 3 (TFF3) peptide [56, 76, 77] and IL-13 has also been shown to induce goblet cell metaplasia in the lung [78]. Although mCLCA3 increases mucus production in lung and intestine, mucins exhibit differential expression in each tissue type (i.e. lung vs. intestine) along with differential expression based on localization of goblet cells within the tissue (i.e. bronchi vs. bronchioles in lung, crypt base vs. villus tip in intestine). Thus, it is not known if mCLCA3 has a regulatory effect on the expression of all mucin species.

I. D. Mucus

The development of mucus is stimulated in the lung by the presence of pathogens, inflammatory mediators and toxins [79, 80] and is stimulated in the intestine by the chemical and antigenic challenges of intestinal microbiota [81]. Mucus acts as the first line of defense for the immune system and is also important in lubrication and transport between the lumen and epithelial lining but this protective role of mucus becomes the major contributor of the CF phenotype, as described in section *I. A. ii*. Goblet cells are responsible for mucus production and these cells maintain a functional mucosal layer in the intestine and lung [82]. They are formed from the proliferation and differentiation of basal multipotential stem cells [82, 83] but can also be formed by trans-differentiation (described in section *I. C. iii* and shown in Figure 1.3) of clara [84, 85] and ciliated cells [86].

The distinct shape of goblet cells (Figure 1.4), resembling a chalice or cup, is mainly determined by the size and shape of the theca. The theca is composed of microtubules and intermediate filaments and its structure acts to encapsulate the mucin

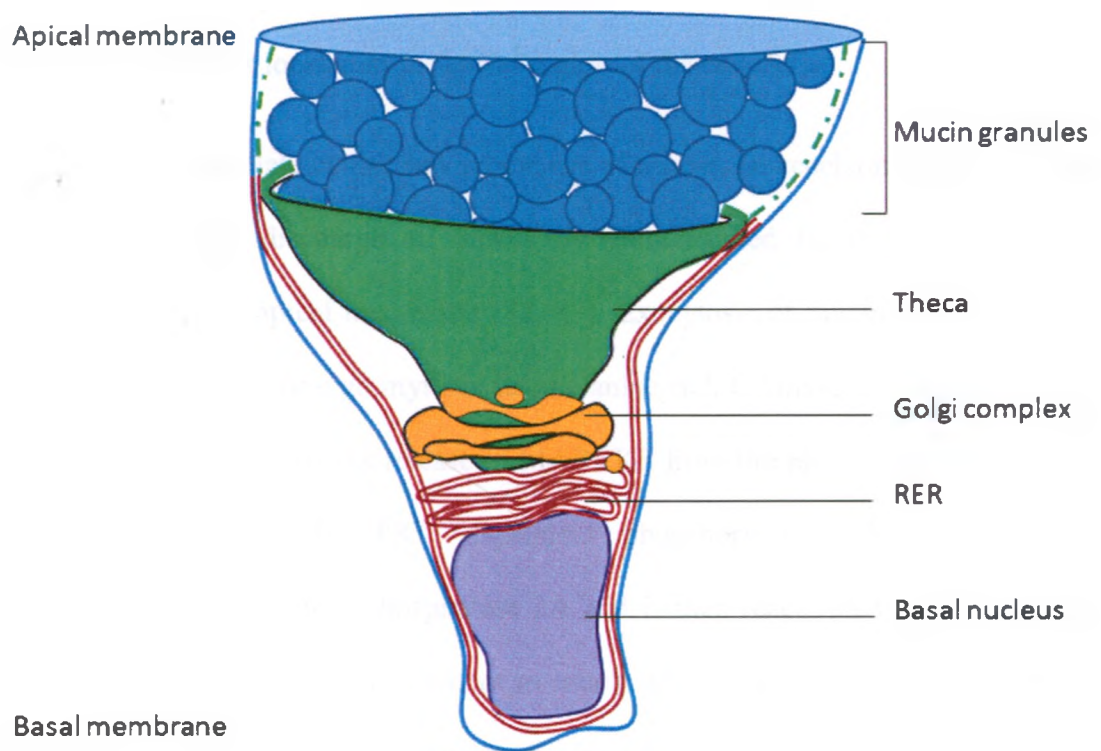


Figure 1.4. General architecture of a goblet cell. Mucin granules, containing condensed mucins, are stockpiled within the theca at the apical region of the goblet cell. The rough endoplasmic reticulum (RER), located in the basal and supranuclear regions of the cell, is responsible for protein synthesis. The Golgi complex, stacked atop the nucleus, is responsible for mucin processing. The polarized structure of the cell allows for unidirectional mucin synthesis and secretion into the lumen, figure adapted from [82].

granules within the goblet cell [82, 87]. After transcription of the mucin genes, the full length protein is synthesized in the rough endoplasmic reticulum, which surrounds the nucleus basolaterally and extends to the supranuclear region of the goblet cell [82, 88]. The Golgi complex, located solely in the supranuclear region, is responsible for mucin protein processing [82]. The mucins are then transported to mucin granules where they are stored until secretion. Basal mucus secretion involves the constitutive exocytosis of select mucin granules located in the apical region of the cell [89].

Irritants stimulate compound exocytosis of mucus, an accelerated secretion where goblet cells rapidly discharge all mucus by uninterrupted fusion of mucin granule membranes with the apical membrane [82, 89]. Exocytosis of mucin granules has been shown to be mediated through myristoylated alanine-rich C kinase substrate (MARCKS) [90]. The mechanism involves release of MARCKS from the plasma membrane into the goblet cell cytoplasm by PKC dependent phosphorylation, MARCKS is then dephosphorylated by protein phosphatase 2A and is then reactivated by PKG mediated phosphorylation enabling its attachment to mucin granule membranes [90]. Binding of MARCKS to the mucin granule membranes allows for the controlled movement of mucin granules within goblet cells to the apical membrane, followed by exocytosis of the mucus contents into the mucosal layer in the lumen. The cup-like shape of goblet cells is maintained following mucin degranulation thanks to the complex three dimensional framework of the intermediate filaments that make up the theca. Following secretory events, mucin production begins to refill the granules of the goblet cells as early as one hour after degranulation [82].

As described previously, mucus plays an important role in immune defence, and normal function of the mucosal layer includes clearance by ciliary motion. Mucociliary clearance requires a balance of mucus volume, mucus composition, periciliary fluid and normal ciliary beat frequency [91]. In CF, additional polymers are present in mucus affecting the fluidity of the mucosal layer. In the lung, bacteria, polymerized DNA from inflammatory cell necrosis, proteoglycans and dead cells contribute to the thick sputum; this overwhelms the normal ciliary function and leads to airway obstruction (reviewed by Voynow *et al.* in [92]). Improper clearance of mucus can lead to infection and tissue scarring [26-29, 31].

I. D. i. Mucins

The viscoelastic properties associated with mucus are in large part due to mucins. Mucins are large glycoproteins with a characteristic trait of having tandemly repeating serine and threonine amino acids which are the sites of glycosylation [80]. Mucin protein translation takes place in the endoplasmic reticulum and N-glycosylation occurs co-translationally. Additional modifications include O-glycosylation, and termination of oligosaccharide chains with sialyl and sulfate groups by sialyltransferases and sulfotransferases, respectively [81, 93, 94]. The oligosaccharide side chains are predominantly made up of five sugars: galactose, fucose, N-acetylglucosamine, N-acetylgalactosamine and sialic acid [95], although other sugars such as mannose and xylose can also be added [96]. Human colonic mucins contain 21 distinct oligosaccharide side-chain structures, of them 10 are acidic in nature and 11 are neutral [82]. Sulfate termination of the oligosaccharide chains leads to inter-mucin chain bonding that leads to dimerization and oligomerization in the Golgi complex.

Mucins are categorized into two structurally distinct groups based on whether they are: membrane associated mucins, containing a transmembrane sequence; or secreted, gel-forming mucins [94, 97]. MUC2, MUC5AC and MUC5B are considered to be the major gel-forming mucins while MUC1, MUC3 and MUC4 are the main membrane-bound mucins (Table 1.1). As previously mentioned, the serine and threonine rich regions located in the central domain are characteristic of all mucin proteins [80] and are the main sites of glycosylation. Depending on the type of glycosyltransferases expressed in the cell, oligosaccharides can account for anywhere from 50-90% of the molecular mass of mucins [98]. The oligosaccharide side-chains on mucins immobilize pathogens on the mucosal layer by emulating glycoproteins present on the epithelial cell membrane[99].

Gene	Mucin Type	Tissue expression
MUC1	Membrane-bound	all secretory epithelial cells
MUC2	Secreted	small and large intestine
MUC3	Membrane-bound	small intestine
MUC4	Membrane-bound	airways, large intestine
MUC5AC	Secreted	airways, stomach
MUC5B	Secreted	airways, submandibular gland

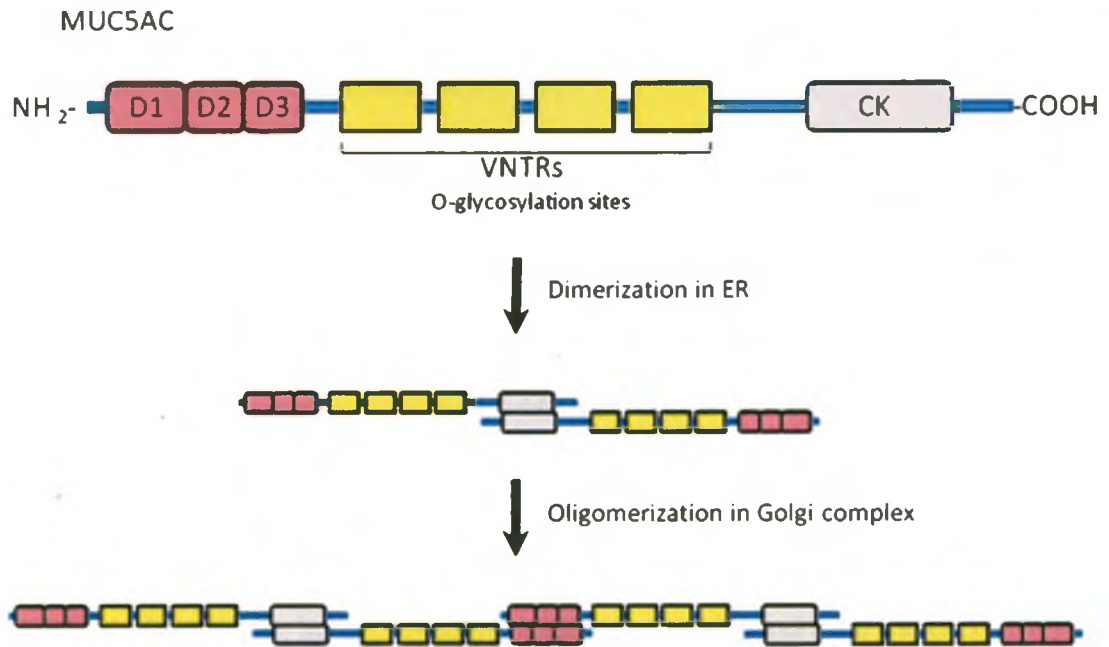
Table 1.1. Expression profile of MUC genes and structure type of mucin proteins. The type of mucin protein structure and the major tissue localization of each of the major MUC gene transcripts are shown. It is possible for MUC expression to occur in other tissues as well, but at much lower levels. Table adapted from [100].

Figure 1.5 shows the proposed structure of the secreted MUC5AC and membrane-bound MUC1. In secreted mucins, disulfide bonding between C-terminal cysteine knot (CK)-like domains causes dimerization in the endoplasmic reticulum that are further connected into oligomers through N-terminal disulfide bonding at D-domains in the Golgi complex (Figure 1.5a) [101]. It is assumed that these large oligomers are composed

of individual species of mucins, but it is possible that heteromeric complexes are also formed. These large oligomers then move into mucin granules for storage and await secretion into the lumen. Repulsion of the negatively charged mucins are shielded by high Ca^{2+} ion concentrations in the mucin granules and allows these large mucins to be highly condensed [93, 101]. Expulsion into the lumen causes Ca^{2+} ions to be replaced mainly by K^+ ions, shielding by this ion exchange is less effective and a phase transition occurs where the mucus balloons in size due to hydration [93, 101]. The oligomers that make up the mucosal layer then provide a three-dimensional network where interaction of luminal molecules with the epithelial layer requires diffusion through the pores of the mucosal network [101-103].

Figure 1.5b shows the structure of MUC1, which shares a similar structure to most membrane-bound mucins. These mucins have transmembrane regions that tether the protein to the cell exterior along with domains called 'sea urchin sperm protein, enterokinase, and agrin' (SEA) modules [97, 98]. SEA domains are common in O-glycosylated environments and are believed to control binding to adjacent carbohydrates [97]. SEA domains present in mucins are cleaved, normally the cleavage site is in close proximity to the transmembrane domain (Figure 1.5b) [97], and then join again via non-covalent bonding [98]. Cleavage of tethered mucins allows for proper glycosylation to occur in the Golgi [80]. Many tethered mucins also contain epidermal growth factor (EGF) domains but their function has not been well established, although it has been suggested that mucin EGF domains may have an effect on mucosal restitution [104]. The best characterized membrane-bound mucins, MUC1 and MUC4, have been shown to localize around the microvilli and cilia on the epithelium and are important components

(a)



(b)

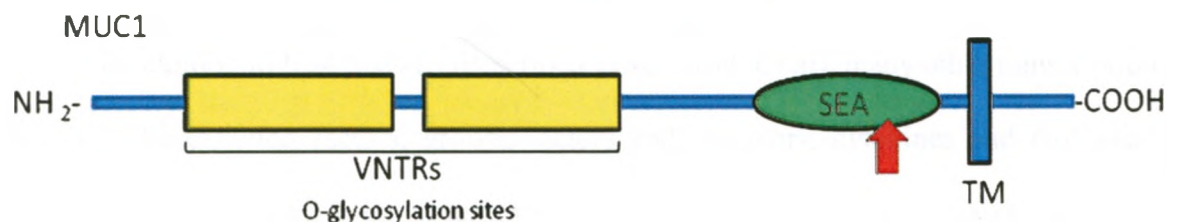


Figure 1.5. Predicted structures of gel-forming and membrane-bound mucins. The variable number of tandem repeats (VNTR), which are Serine, Threonine and Proline rich regions, are heavily O-glycosylated. **(a)** Predicted structure of MUC5AC based on cDNA sequence and structural prediction programs. Inter-chain disulfide bonds form between Cysteine Knot (CK)-like domains, forming mucin dimers in the endoplasmic reticulum (ER). D-domains are underglycosylated regions thought to connect with other mucin dimers through inter-chain disulfide bonds, forming oligomers of various sizes in the Golgi complex. Figure adapted from [101]. **(b)** Predicted structure of MUC1 based on cDNA sequence and structural prediction programs. Transmembrane (TM) domain shows the putative region where MUC1 tethers itself to the extracellular membrane. Sea urchin sperm protein, enterokinase, and agrin (SEA) modules are extracellular domains associated with O-glycosylation and are thought to regulate binding to neighbouring carbohydrates. SEA containing mucins undergo cleavage close to the TM domain (red arrow) and re-associate via non-covalent bonding. Figure adapted from [97, 98].

of the periciliary fluid [98, 105]. In addition to the protective and hydrating effects on the mucosal layer, tethered mucins are also involved in signalling and can help repair a loss of polarized epithelial cell architecture [106].

Expression profiles show that mucin genes exhibit tissue specificity. MUC1 appears to be universally expressed among secretory epithelial cells in humans, while MUC2, -3 and -4 are predominantly expressed in the intestine (Table 1.1). MUC4 is also expressed in the lung along with MUC5AC and -B (Table 1.1). The link between tissue specificity and regulation of MUC gene expression has not yet been established, but MUC1 has been recognized as a cancer marker, where overexpression has been frequently observed in breast, ovarian, lung, colon and pancreatic cancers [107]. This suggests a necessary role for specific mucin regulation in these tissues.

In addition to IL-4 and -13 (described in section *I. C. iii*), many other transcription factors, differentiation factors, growth factors and receptors, cytokines and biological agents have been shown to either up- or down-regulate mucin gene expression, reviewed by Voynow *et al.* in [92] and by Theodoropoulos *et al.* [94]. Regulation of mucins can also occur at the post-translational level as demonstrated by studies on the rat Muc4 protein. Muc4, a protein produced in the rat colon and mammary gland [108], is cleaved into two subunits in the ER. Transforming growth factor beta (TGF- β) represses this processing step thus blocking the synthesis of mature Muc4 protein in the ER [109]. Improper processing of other secreted mucins is likely possible through similar methods and normal processing of membrane-bound mucins is very significant, as cleavage of tethered mucins is required for proper glycosylation of the protein [80]. Although there is heterogeneity of mucin expression and oligosaccharide processing, the various factors

that influence mucin regulation at the transcriptional level (and also post-transcriptionally) show the importance of proper regulation of the quantity and composition of mucus and the subsequent effects on cellular and mucus functional properties.

I. D. ii. Trefoil Factors

The mammalian trefoil factor family contains three members, TFF1, TFF2 and TFF3 [110] which all contain a trefoil domain. TFFs, which have an important role as signalling peptides involved with wound healing, are expressed and secreted by cells that line the mucus-coated epithelium of the GI tract, gall bladder and in salivary glands (Table 1.2). The trefoil domain, a conserved sequence of 38-39 amino acids, contains six cysteine residues with spacings that form disulfide bonds in a 1-5, 2-4 and 3-6 arrangement (Figure 1.6) [111]. TFF1 and -3 contain a single trefoil domain and form homodimers, while TFF2 contains two trefoil domains and the monomer forms a “natural dimer” on its own, reviewed by Thim *et al.* in [112]. Functional activity of TFFs have been studied and in general, TFF dimers have higher activities than the monomers [112] except for TFF3, where inconsistent results have shown the peptide’s variable activities [113]. TFFs are resistant to protease degradation, a vital characteristic which allows the peptides to remain functional in harsh environments [114].

Expression Site	Expression Levels		
	TFF1	TFF2	TFF3
Salivary Glands	low	trace	high
Stomach	high	high	none
Small Intestine	high	high	high
Large Intestine	high	none	high
Gall Bladder	low	low	low

Table 1.2. Expression profile of TFFs. TFF1 is produced mainly in the stomach; TFF2 is produced mainly in the stomach and duodenum of the small intestine; and TFF3 is produced throughout the intestine and salivary glands. Table adapted from [115].

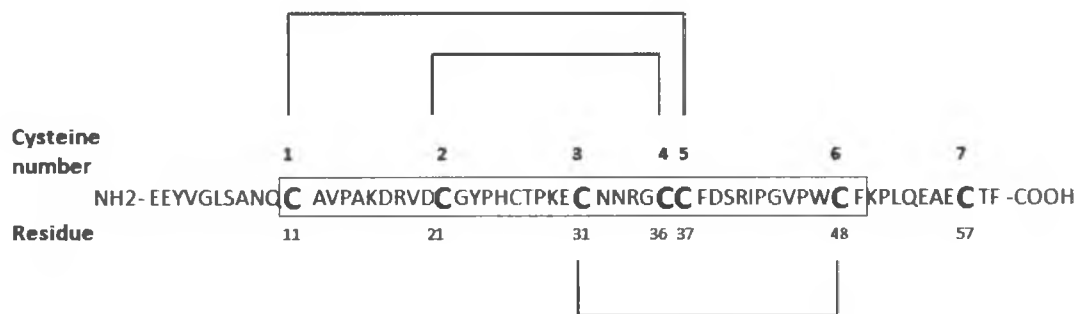


Figure 1. 6. Amino acid sequence of TFF3. The primary sequence of TFF3 signalling peptide is shown, with trefoil domain sequence from residues 11-49 in the red box. The residue number and cysteine number is labeled for each cysteine, along with the 1-5, 2-4 and 3-6 disulfide bonding pairs that form 3 distinct loop structures. The seventh cysteine residue is responsible for the disulfide bond between TFF3 homodimers. Figure adapted from [114].

Trefoil proteins have been found to have an essential role in mucosal restitution as their expression is rapidly upregulated in regions of mucosal injury [116-119]. The protective effects of TFFs include establishment and maintenance of the mucosal layer, improvement of rapid mucosal repair by cell migration (restitution), regulation of mucosal differentiation and regulation of the mucosal immune response [120]. Restitution after injury is essential because it limits the loss of fluid and prevents luminal bacteria or foreign antigens from invading and adhering to the epithelial layer. Restitution can be moderated by numerous factors like: EGF, HGF and TGF- α (reviewed by Taupin *et al.* in [121]) but TFF peptides are thought to have an essential role in the process of restitution at the mucosal layer. Knockout mice deficient in any of the three TFFs have shown abnormalities of the mucosal layer, either through increased susceptibility to injury or the development of antropyloric adenomas that can progress to carcinomas [122-124].

It has been shown that restitution, and normal colonocyte homeostasis, requires TFF3 signalling via the MEK-ERK pathway and this can be carried out by either the TFF3 monomer or the dimer [114]. The importance of the TFF3 dimer was established in the anti-apoptotic effects of TFF3 signalling, which required the peptide dimer in order to activate the PI3K and EGF-R signalling pathways that prevented apoptosis during injury [114]. It has also been shown that induction of STAT3 phosphorylation by IL-6 induced TFF3 expression and promoted biliary epithelial cell proliferation and migration in response to wound healing [125]. This suggests that TFFs are involved in a variety of interactions in order to regulate proper maintenance of the mucosal layer.

Large amounts of TFF3 (a.k.a. intestinal trefoil factor, ITF) can be found within the theca of goblet cells [121]. TFF3 is secreted onto the mucosal layer throughout the

intestinal tract where it co-localizes with MUC2 [126]. TFF interaction with mucins is considered to regulate mucosal layer properties and trefoil factors are commonly co-secreted with various mucins [127]. As an essential regulator of the intestinal mucosal layer, TFF3 expression may be affected by mCLCA3 levels which could help to explain changes in mucin expression, mucus production and mucus secretion.

I. E. Thesis Introduction

mCLCA3 has been shown to have an intimate association with goblet cells, specifically the membranes of the mucin granules [60]. Upregulation of the mCLCA3 gene demonstrated amelioration of the CF phenotype in the intestine of UNC·B6 (-/-) mice [73]. This supports the idea that mCLCA3 is a genetic modifier of CF. Despite its intimate association with mucin granule membranes, mCLCA3 cleavage products are secreted into the luminal mucus as a globular protein [64, 73]. Studies have shown that goblet cell hyperplasia, metaplasia and goblet cell hypertrophy is associated with mCLCA3 overexpression [68, 71, 73], but it is still not entirely clear what role mCLCA3 has on goblet cell development and/or differentiation. mCLCA3 may be responsible for altering the viscosity or rheology of mucus through altered mucin gene expression or down-regulation of mucin degranulation in goblet cells.

Due to its obvious role in affecting the production of specific mucins and inducing goblet cell hyperplasia and/or metaplasia in murine intestine and lung, the objective of this study was to determine how mCLCA3 overexpression affects the synthesis, composition, processing and secretion of mucins within goblet cells. This study also wanted to examine mCLCA3's role in the morphometry of goblet cells in culture. **The**

hypothesis is that upregulation of the mCLCA3 gene in the HT29 cell line leads to differential synthesis, processing and secretion of mucus/mucin proteins, while also having an adjuvant role in the proliferation or development of goblet cells. The connection between mucins, TFFs and mCLCA3 needs to be elucidated as it can potentially be significant in CF and other mucous-based diseases. To address the hypothesis, this study will investigate the role of mCLCA3 with respect to mucus production and goblet cell physiology in HT29 cell cultures using RT-PCR, qPCR, western blots and histological staining.

II. Materials and Methods

II. A. HT29 cell culture and butyrate treatment

II. A. i. Cell culture media, passage, cryopreservation and revival:

With the exception of cells cultured in the presence of sodium butyrate and the recovery growth phase after removal of sodium butyrate from the medium (explained below), all cells were grown in sterile, pre-warmed (at 37°C) Dulbecco's Modification of Eagle's Medium (DMEM) (Wisent #319-020-CL) with 10% fetal bovine serum (FBS) (Wisent #080150), 100 mM sodium pyruvate, 40 mM L-glutamine, 100 µg/mL streptomycin, 0.25 µg/mL amphotericin B and 100 IU/mL penicillin. Stably transfected cells were grown in DMEM with 10% FBS, 100 mM sodium pyruvate, 40 mM L-glutamine, 100 µg/mL streptomycin, 0.25 µg/mL amphotericin B, 100 IU/mL penicillin and G418 (Wisent #400-130-IG) at a final concentration of 600 µg/mL. The cells were maintained at 37°C in 5% CO₂ in air, and were fed with complete growth medium with 10% FBS every 2-3 days until they reached 70-80% confluence.

When the adherent HT29 human adenocarcinoma colonic epithelial cell line and its derivatives reached 70-80% confluency, they were rinsed twice with sterile, calcium-magnesium free Dulbecco's phosphate-buffered saline (PBS) (Wisent #311-425-CL) to remove any residual serum. The cells were detached from the plate by incubating with 2 mL of pre-warmed 0.25% trypsin 0.1% EDTA solution (Wisent #325-043-EL) for 5 min at 37°C in a 10 cm diameter Petri dish. For 6-well plates, 400 µL of trypsin-EDTA was used per well whereas 200 µL of trypsin-EDTA was used per well for 24-well plates. After cell detachment, trypsin was inactivated by the addition of an equivalent amount of

complete growth medium containing 10% FBS, followed by disaggregation of the cell layer by repeated gentle pipetting. Cells were then seeded in 1:10 ratios into new culture vessels. Each culture vessel was gently swirled to help evenly distribute the cells and each vessel was maintained at 37°C in 5% CO₂ in air.

For storage, when all cell line derivatives reached 70-80% confluency in Petri dishes, they were washed twice with 10 mL of pre-warmed PBS and detached with 2 mL of pre-warmed trypsin-EDTA for 5 min at 37°C. An aliquot of 2 mL complete growth medium was added and mixed with each plate. The cells were then removed, centrifuged at 61.5 x g for 5 min at 4°C. The supernatant was discarded and the pellet was resuspended in 5 mL ice cold cryoprotectant media (95% complete growth medium: 5% DMSO). Stably transfected cells were resuspended in 5 mL of cryoprotectant medium under G418 drug selection (complete growth medium with 600 µg/mL G418, 95%: DMSO, 5%). Cell aliquots of 1 mL in cryoprotectant media were pipetted into ice cold cryotubes. The cells were then frozen at -20°C for 2 hours, then at -80°C overnight. The following day all cells were transferred to -150°C for long-term storage.

To thaw frozen cells, they were taken from -150°C and rapidly thawed in a 37°C water bath with gentle agitation. The vial contents were transferred to a 15 mL centrifuge tube containing 9 mL of pre-warmed complete growth medium. The tubes were spun down at 61.5 x g for 5 min to remove the DMSO. The supernatant was discarded and the cell pellet was resuspended in 10 mL of appropriate pre-warmed complete growth medium and was dispensed into a Petri dish.

II. A. ii. Sodium butyrate treatment:

The chemically differentiated cell line (HT29-d) was produced using sodium butyrate (NaBt) as per Augeron and Laboisse [128] with the intent of obtaining a cell line high in goblet cell population similar to the HT29-Cl.19E line established in this paper. Differentiation of the HT29 cell line was induced by adding sodium butyrate (Alfa Aesar #AAA11079-22), to a final concentration of 5 mM, to the complete growth medium. NaBt treatment of HT29 cells was performed in 3 stages: in stage 1 the cells were normally subcultured at day 1 and the growth medium containing 5 mM NaBt was introduced at day 3 and was changed every 2 days until day 11. In stage 2 the cells were treated with trypsin-EDTA solution and divided equally into three plates, with the 5 mM NaBt containing growth medium changed every 2 days until day 25. In the final stage, stage 3, the cells were briefly treated with trypsin-EDTA and the dissociated cells were discarded. The remaining bound cells were treated once again with trypsin-EDTA, recovered and seeded at approximately 200 cells per Petri dish. These cells were grown during a 28 day recovery phase in a 1:1 (v/v) of DMEM: Ham's F-12 Mix (Wisent #319-075-LL) with 10% FBS, 100 mM sodium pyruvate, 40 mM L-glutamine, 100 µg/mL streptomycin, 0.25 µg/mL amphotericin B and 100 IU/mL penicillin. After the stage 3 recovery phase was finished, individual colonies were selected using cloning rings and trypsin-EDTA. Each colony was seeded to a single well in a 24-well plate. When each well reached 70-80% confluency, they were treated with trypsin-EDTA and seeded to 6-well plates. To determine the extent of goblet cell proportion to the total cell population, HT29 and HT29-d cells were cultured 18 days past confluency. Goblet cell counts were

performed after cultures were stained using alcian blue, pH 2.5 and counterstained using 0.1% nuclear fast red, described in detail in section II. E.

II. B. mCLCA3 plasmid construction and transfection

II. B. i. Construction of pBS KS+ mCLCA3 plasmid:

Total RNA was collected from wild-type B6 mouse ileum using the RNeasy Mini Kit (QIAGEN #74104). Collected tissue was preserved in RNAlater Stabilization Solution (Sigma-Aldrich #R0901) to prevent nucleic acid degradation. RNAlater solution inhibits the activity of RNAses and DNAses during cell lysis and was used to preserve mRNA transcripts during total RNA sample collections. All tissue samples were stored at -80°C. Tissue aliquots of 30 mg were disrupted in 300 µL RLT buffer with 1% β-mercaptoethanol (β-ME). The sample was homogenized using a handheld homogenizer for 10 seconds. This was followed by the addition of 300 µL 70% ethanol to promote selective binding of the RNA to the column membrane, and then the solution was transferred to an RNeasy spin column. Contaminants were washed away using the appropriate buffers provided in the kit. The RNA was eluted from the column in two centrifugation steps; with an initial volume of 30 µL RNase free water followed by another 20 µL of RNase free water. Total RNA samples were stored at -80°C.

Total RNA (1 µg) was thawed on ice and treated with 2 µL of DNase I (Sigma-Aldrich #AMPD1-1KT) for 15 min at room temperature. The DNase I was heat inactivated along with the addition of 2 µL of Stop Solution (Sigma-Aldrich #AMPD1-1KT) at 70°C for 10 min. Samples were chilled and centrifuged before reverse transcription. Appropriate buffers were added, as per manufacturer's protocol, and

samples were then treated with Superscript II Reverse Transcriptase (Invitrogen #18064-014) for 10 min at 25°C, then at 42°C for 50 min and were then heat inactivated at 70°C for 15 min. -RT samples were treated under the same conditions and with the same reagents as +RT samples, but no Superscript II Reverse Transcriptase was used on these samples. To remove any residual RNA, 1 μ L RNase H (Invitrogen #18021-014) was added to each tube and incubated at 37°C for 20 min. The cDNA was stored at -20°C until ready for PCR.

The complete mCLCA3 gene was amplified using 0.5 μ L of first strand cDNA template from UNC·B6^{+/+} ileal tissue, 1 μ L of mCLCA3-XhoI F primer at 100 ng/ μ L (Table 2.1), 1 μ L of mCLCA3-XhoI R primer at 100 ng/ μ L (Table 2.1) and 22.5 μ L of Accuprime Pfx Supermix (Invitrogen #12344-040). Four reaction tubes of +RT cDNA and one reaction tube of -RT cDNA were used. Thermal cycling was performed for 40 cycles (94°C denaturing step for 30 sec, 62°C annealing step for 1 min, 72°C elongation temperature for 2 min followed by a final elongation step at 72°C for 10 min) using the DNA Engine Tetrad 2 Cyler (Bio-Rad Laboratories). The PCR products were electrophoresed on an ethidium bromide stained 0.8% agarose gel at 100V for 2 hours and the DNA bands were visualized under UV light. The DNA band at 2.9 kb was excised from the gel using a clean razorblade and weighed.

The PCR product at 2.9kb was cleaned using the QIAquick Gel Extraction Kit (QIAGEN #28704). The weighed gel slice containing the mCLCA3 DNA band was melted, cleaned and isolated using the QIAquick column and appropriate buffers as per the QIAGEN protocol. The DNA was eluted from the column in 35 μ L of 10 mM Tris·HCl, pH 8.5.

The purified XhoI-flanked mCLCA3 DNA and the pBluescript KS+ (pBS KS+) vector were digested with the restriction enzyme XhoI at 37°C for 2 hours. The pBS KS+ vector was also treated with Calf Intestinal Alkaline Phosphatase (CIAP) (Invitrogen #18009-019) for an additional 15 min at 37°C after XhoI digestion, this was done to help reduce self-ligation of the vector. The mCLCA3 cDNA and the CIAP treated pBS KS+ vector were run on an ethidium bromide stained 0.8% agarose at 100V for 2 hours. The mCLCA3 and pBS KS+ bands were visualized under UV, excised from the gel and were cleaned using the QIAquick Gel Extraction Kit (detailed above). Ligation of the mCLCA3 insert and the pBS KS+ vector was performed by first incubating 165 ng of XhoI-treated mCLCA3 with 30 ng of XhoI-CIAP-treated pBS KS+ in a microcentrifuge tube at 65°C for 5 min. The tube was chilled and spun down and the insert and vector were ligated using T4 DNA Ligase (Invitrogen #15224-025) at room temperature for 1.5 hours.

XL-10 Gold Ultracompetent Cells (100 µL) (Stratagene #200314) were transformed with 1 µL of the ligation mixture. The thawed XL-10 Gold cells were transferred to a pre-chilled 14 mL round-bottom tube on ice. An aliquot of 4 µL β-ME mix was added and incubated on ice for 10 min with gentle swirling every 2 min. An aliquot of 1 µL of the ligation mixture was added to the cells and incubated on ice for 30 min. The cells were then heat-pulsed in a 42°C water bath for 30 sec and incubated on ice for 2 min. An aliquot of 900 µL of SOC-medium (Invitrogen #15544-034) was added to the cells and the tube was incubated at 37°C for 1 hour with shaking at 225 rpm. The cells were plated at 1:10, 1:50, and 1:100 dilutions onto LB agar plates. The cells were incubated on inverted LB agar plates (with 100 µg/mL ampicillin) overnight at 37°C (16

hours). All of the steps for transforming the XL-10 cells were carefully performed next to an open flame to prevent contamination of the LB- or SOC-growth media.

Blue-white colour screening was used to compare colonies picking up plasmids with and without inserts. After the LB agar plates solidified, 100 μ L of 10 mM IPTG and 100 μ L of 2% X-gal were mixed into a 100 μ L pool of SOC medium and the mixture was spread across each plate. After removing the plates from 37°C the next morning, colour screening was enhanced by placing the plates in 4°C for 2 hours. Colonies containing plasmids with inserts were white and colonies containing plasmids without inserts were blue; 15 single white colonies were picked to inoculate 15 starter cultures of 3 mL LB with 100 μ g/mL ampicillin.

Plasmid minipreps were performed using the QIAprep Spin Miniprep Kit (QIAGEN #27104) as per the manufacturer's protocol. To harvest the bacterial cells for the miniprep, 1.5 mL of cell culture was centrifuged at 5800 x g for 3 min at room temperature. The supernatant was discarded and the bacterial pellet was resuspended, lysed and neutralized. After removal of the cell debris by centrifugation, the supernatant was applied to the QIAprep spin column. The DNA was washed and then eluted in 50 μ L of 10 mM Tris·Cl, pH 8.5.

After the plasmid miniprep, restriction enzyme mapping was performed on each plasmid to verify the correct sized insert was present. Each plasmid was treated with KpnI (which has a single cut site in the pBS KS⁺ vector) at 37°C for 1 hour and was run on a 0.8% agarose 1% TAE gel at 100V for an hour to verify the plasmid was of the

approximate 5.9 kb size. After this initial screen, plasmids were mapped using several restriction enzymes to verify positive clones.

The inserts within the plasmids of positively mapped clones were sequenced for verification. The mCLCA3 insert was sequenced using the following primers (Table 2.1): mCLCA3#3, mCLCA3#4 and Gob5#16 along with the standard T7 promoter and T3 primers provided by the Robarts Research Institute, University of Western Ontario. A plasmid that contained only a single basepair error (silent mutation not affecting translation) within the coding region was selected. The colony containing this plasmid was used to inoculate a starter culture of LB.

Plasmid maxipreps were then performed using the QIAGEN Plasmid Maxi Kit (QIAGEN #12162) as per the manufacturer's protocol. To harvest the bacterial cells for the maxiprep, 250 mL of cell culture was centrifuged at 6000 x g for 15 min at 4°C. The supernatant was discarded and the bacterial pellet resuspended, lysed and neutralized. After removal of cell debris by centrifugation, the supernatant was applied to the QIAGEN-tip 500 column. The DNA was washed and then eluted in 15 mL 1.25 M NaCl; 50 mM Tris·Cl, pH 8.5, 15% isopropyl alcohol (v/v). The DNA was precipitated by adding 10.5 mL of 100% isopropyl alcohol and centrifuged at 15000 x g for 10 min at 4°C. The DNA pellet was air dried and redissolved in 500 µL of 10 mM Tris·Cl, pH 8.5. The plasmid was split into 5 x 100 µL aliquots and stored at -20°C.

II. B. ii. Construction of pDream2.1-mCLCA3 plasmid:

The mCLCA3 insert (Gene NM_017474) was subcloned from the pBS KS+ mCLCA3 plasmid into the pDream2.1-MCS vector (Genscript #SD0222) via the BamHI

and HindIII sites (Figure 2.2). Subcloning was performed by GenScript USA. The insert of the pDream2.1- mCLCA3 plasmid was sequenced and verified for correct sequence and orientation with respect to the CMV promoter. The pDream2.1-mCLCA3 plasmid and empty pDream2.1-MCS vector were each transformed into XL-10 Gold Ultracompetent Cells and a maxi prep was performed for each as described above.

II. B. iii. Transfection of HT29 cultures using pDream2.1-mCLCA3 plasmid:

Transient transfection was performed using calcium phosphate co-precipitation on HT29 cells. A 90% confluent plate of cells was split at 1:20 the day before transfection. The two buffers used for transfection; 2X HEPES buffer (280mM NaCl, 50 mM HEPES, 1.5 mM NaPO₄, pH 7.0) and 2 M CaCl₂ were sterilized by filtration. Transfecting a 10 cm² dish of HT29 cells, 10 µg of plasmid was added to 61 µL of 2 M CaCl₂ and dH₂O was added to a final volume of 0.5 mL. This was added drop-wise to 0.5 mL of 2X HEPES buffer and mixed. The mixture was incubated for 30 min at room temperature to allow for precipitate formation. The precipitated solution was mixed and then pipetted on top of cultured cells on serum-free, antibiotic-free DMEM. The dish was gently swirled and returned to 37°C in 5% CO₂ in air overnight. The following day, the medium was replaced with complete DMEM. The pDream2.1-mCLCA3 plasmid was used for this experiment (HT29trCLCA3) and the empty pDream2.1-MCS vector was used as the negative control (HT29trMCS). In addition to the empty pDream2.1-MCS vector, HT29 cells were treated using the calcium phosphate transfection mixture without plasmid/DNA as a negative control (HT29-CaP).

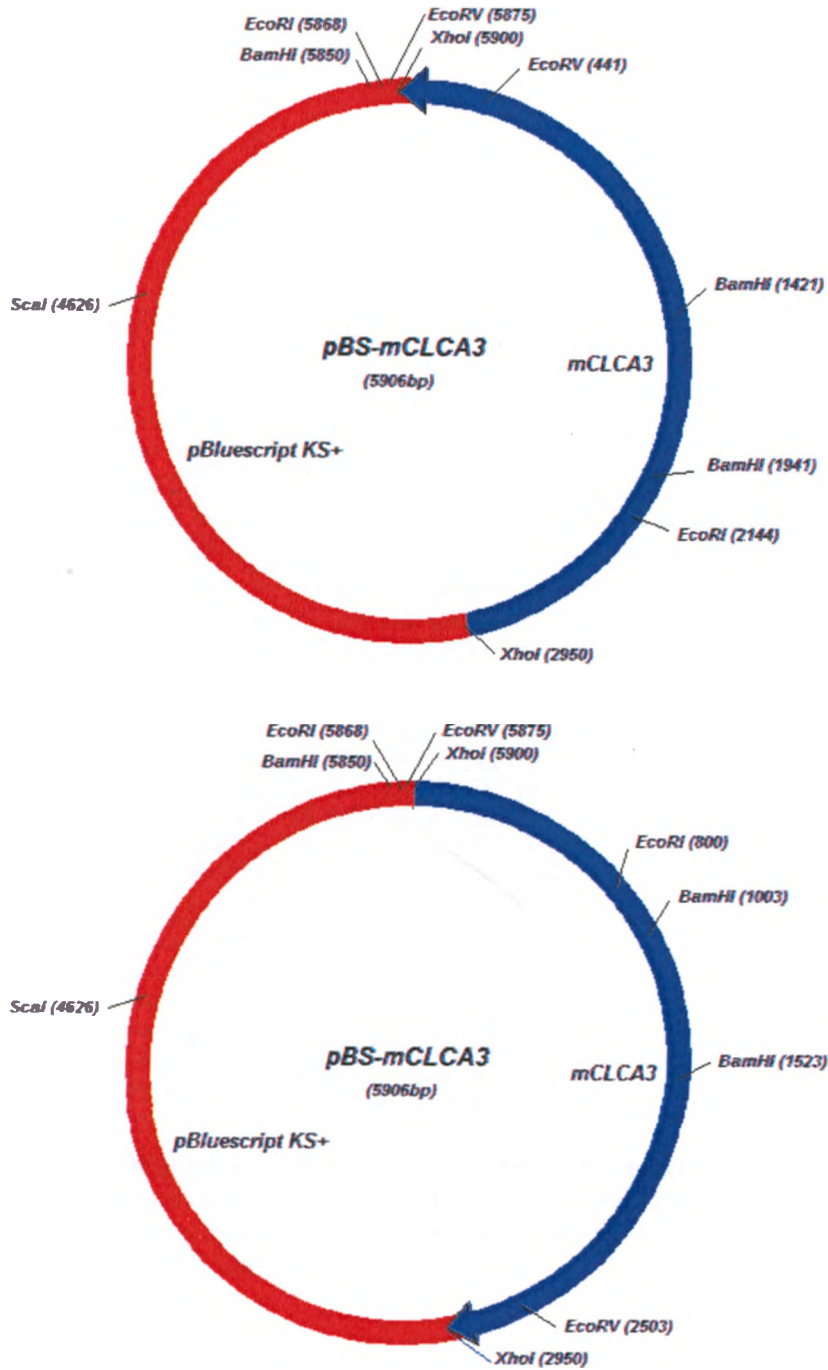
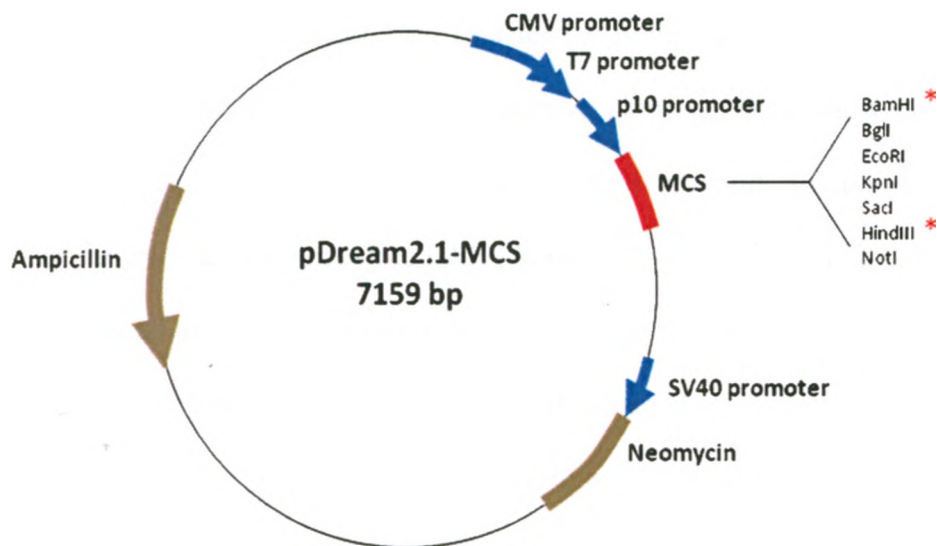


Figure 2.1. pBS-mCLCA3 plasmid constructs. Purified mCLCA3 amplified from UNC-B6^{+/+} ileal mouse tissue was cloned into pBS-KS⁺ vector via the *XhoI* site. Restriction enzyme sites used for mapping the plasmid and verifying gene orientation are also shown.

Primer Name	Primer Sequence (5' → 3')	PCR Conditions (if applicable)		
		Annealing Temp.	Elongation Temp.	Cycle #
mCLCA3-1F	Fwd: ATG GAA TCT TTG AAG AGT CCT GTC	62°C	72°C	40
mCLCA3-1R	Rev: TCA GTG CAA ACC TAG TGT CAC C			
mCLCA3-Xho1F	Fwd: AAA GCT CGA GGA TGG AAT CTT TGA AGA GTC CTG TCT ICC	62°C	72°C	40
mCLCA3-Xho1R	Rev: GAT TTC TCG AGT GAA AAT TCA GTG CAA ACC TAG TGT CAC CTG			
mCLCA3 #3	Fwd: GGA ATC TGA GGA CTT CAA G	-	-	-
mCLCA3 #4	Rev: ACC ATT TTG TTC CAC TCC GCT G	-	-	-
Gob5 #15	Fwd: TTC AGC AGG ACA TCT TCA GG	69°C	78°C	35
Gob5 #16	Rev: TTC CTC AGA GCT GGC CTC TTT G			
B-Actin #190-03	Fwd: TCG TGG GCC GCT CTA GGC ACC A	60-71°C	78°C	-
B-Actin #190-04	Rev: GTT GGC CTT AGG GTT CAG GGG GG			
MUC1-F	Fwd: GAT ACC TAC CAT CCT ATG AGC GAG	68°C	78°C	40
MUC1-R	Rev: ACT GCT GGG TTT GTG TAA GAG AGG			
MUC2#3	Fwd: CAG GAT GGC GCC TTC TGC TA	60°C	78°C	40
MUC2#5	Rev: ATG CTG CTC CAA GCT GAG GT			
MUC3B-F	Fwd: TTG ACT ACA ACC ACA GAC CTT CCC	68°C	78°C	40
MUC3B-R	Rev: TGA AGA GTG GAC GTA GAG GAA TCC			
MUC5AC-F	Fwd: GCC CCT TGT TCT GTG ACT TCT ACA	66°C	78°C	40
MUC5AC-R	Rev: GTG TGG TAG ATG ACG TCC TGG TAG			
MUC5B-F	Fwd: ACA GCT ACC AGC TTT ACA GCC ATC	71°C	78°C	40
MUC5B-R	Rev: AGT ACC ACT GGT CTG TGT GCT AGA			
TFF3-F	Fwd: AGT GCC TTG GTG TTT CAA GC	69°C	78°C	40
TFF3-R	Rev: GCA AAG GGA CAG AAA AGC TG			
T7 promoter	TAA TAC GAC TCA CTA TAG GG	-	-	-
T3 promoter	ATT AAC CCT CAC TAA AGG GA	-	-	-

Table 2.1. Oligonucleotide Primers used for PCR experiments and DNA sequencing. Primers were designed using the OligoPerfect Design program (Invitrogen) with a salt concentration of 50mM. PCR conditions apply to primer-sets used for RT-PCR and qPCR. Primer sequences for MUC2 gene from [129].

(a)



(b)

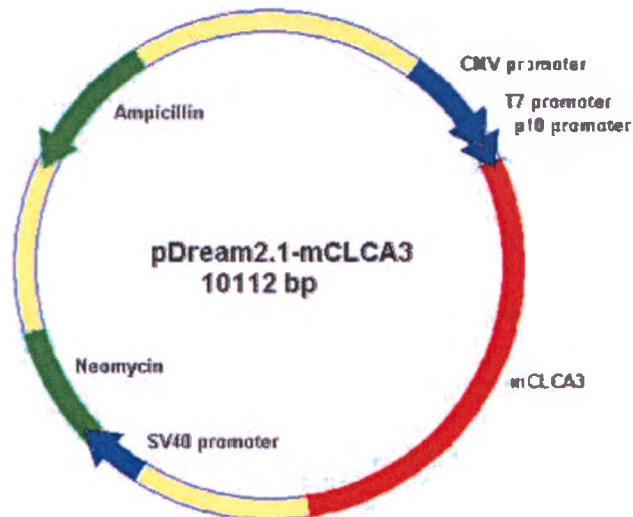


Figure 2.2. pDream2.1-MCS vector map and pDream2.1-mCLCA3 plasmid construct. (a) pDream2.1-MCS expression vector (GenScript) used for subcloning of mCLCA3 gene from pBS-mCLCA3 plasmid, Figure 2.1, into the Multiple Cloning Site (MCS) via BamHI and HindIII sites (b) Construct of the pDream2.1-mCLCA3 plasmid used for transfecting the mCLCA3 gene into HT29 cells.

Stable transfection was performed using Lipofectamine 2000 (Invitrogen #11668-027). HT29 cell cultures grown in 6-well plates were transfected using this method. Two solutions were prepared for the transfection of the pDream2.1-mCLCA3 plasmid (and the pDream2.1-MCS vector for the negative control). Solution A consisted of 99 μ L of serum-free, antibiotic-free DMEM and 2 μ g of plasmid. Solution B consisted of 97.5 μ L of serum-free, antibiotic-free DMEM and 4 μ L of Lipofectamine 2000. This solution was incubated at room temperature for 5 min. After this incubation period, Solutions A and B were combined, mixed and allowed to incubate at room temperature for 20 min for lipid-DNA complex formation. During this time, 95% confluent cells were washed with 2 mL of DPBS and 0.6 mL of serum-free, antibiotic-free DMEM was added to each well. Lipid-DNA complex solution (200 μ L) was slowly overlaid to each well and the dish was gently swirled. The cells were incubated at 37°C in 5% CO₂ for 4 hours, then 0.8 mL of DMEM with 10% FBS was added to each well. The next day, the medium was replaced with 2 mL of complete DMEM with 10% FBS. Two days after transfection, complete growth medium was replaced with complete DMEM with 10% FBS supplemented with 600 μ g/mL of G418 for selection. Medium was exchanged every 2 days for 2 weeks. Each colony was isolated using cloning rings and passaged separately into 24-well plates with drug selection. When clones reached about 80% confluency, they were passaged into 6-well plates with drug selection and screened using RT-PCR.

II. C. mCLCA3 RNA expression

Total RNA was collected from cell cultures using the GenElute Mammalian Total RNA Miniprep Kit (Sigma-Aldrich #RTN70). Cells grown in 6-well plates were harvested using 250 μ L of Lysis Solution with 1% β -ME. Cellular debris was removed

and DNA was sheared by centrifugation through a GenElute Filtration Column. An aliquot of 250 μ L of 70% ethanol was added to the filtered lysate to promote selective binding of the RNA to the column membrane and the solution was transferred to a GenElute Binding Column. Contaminants were washed away using the appropriate buffers provided in the kit. The total RNA was eluted from the column in 50 μ L of Elution Solution and samples were stored at -80°C .

cDNA synthesis of cell culture total RNA was performed as described in *II. B. i*.

II. C. i. Reverse transcription PCR:

RT-PCR experiments were performed in the DNA Engine Tetrad 2 Peltier Thermal Cycler. RT-PCR was used to determine optimal annealing temperatures for primer-sets by performing temperature gradients. Cycling programs had an initial denaturation step of 94°C for 3-5min, followed by 35 cycles of 94°C (denaturation step) for 30 sec, $60-71^{\circ}\text{C}$ (annealing step) for 30 sec and 78°C (elongation step) for 30 sec with a final elongation step at 78°C for 5 min (Table 2.1). PCR products were run on an ethidium bromide stained 1.5% agarose 1% TAE gel at 100V gel for 45 min and visualized under UV light.

RT-PCR was also used to verify mCLCA3 expression in transfected cell lines, both stable and transient, before analysis by quantitative real-time PCR.

II. C. ii. Quantitative real-time PCR:

Comparative quantification was performed using the Stratagene Mx300P System and Perfecta SYBR Green SuperMix, Low ROX (Quanta Biosciences Inc. #CA101414-

166). Primer sets specific for mCLCA3, MUC1, MUC2, MUC3B, MUC5AC, MUC5B and TFF3 were used to determine relative expression levels of these genes in each cell line. Primer concentrations were optimized for each primer-set so as to minimize background (Table 2.2). Primer concentrations ranging from 100-400 ng/ μ L (in 100 ng/ μ L increments) were used to ensure minimal background bands and to maximize amplification of the desired gene product.

To ensure cDNA was not contaminated, standard curves were performed on diluted cDNA samples and respective –RT samples were used as negative controls. Dissociation curves of samples with a sharp peak and lack of amplification in the –RT ensured that cDNA samples were free of contamination and suitable for comparative quantification reactions.

Primer Name	Concentration (ng/μL)
Gob5#15	400
Gob5#16	400
MUC1-F	400
MUC1-R	400
MUC2#3	100
MUC2#5	300
MUC3B-F	300
MUC3B-R	400
MUC5AC-F	400
MUC5AC-R	400
MUC5B-F	400
MUC5B-R	400
TFF3-F	400
TFF3-R	300
B-Actin #190-03	25
B-Actin #190-04	25

Table 2.2. Primer concentrations used for Real-Time PCR analysis. Additional details of PCR conditions for each primer-set are described in Table 2.1.

Comparative qPCRs were performed on HT29, HT29-CaP, HT29trMCS and HT29trCLCA3 isolated samples. β -actin was used as the reference product for each cDNA sample and amplification of each target gene was normalized to β -actin amplification. No template controls were used as negative controls to ensure PCR master-mixes were not contaminated with DNA.

II. D. mCLCA3 protein expression

II. D. i. Total protein collection and quantification:

Total protein was collected from cell cultures 18 days post-confluency. Cells were serum-starved for 24 hours before lysis in lysis buffer (7.5 mL of 150 mM NaCl, 12.5 mL of 50 mM Tris-HCl, 1 mL of 2 mM EDTA, 2.5 mL of Triton X-100 and 2.5 mL of NP-40 with dH₂O added to a final volume of 250 mL). Before using the lysis buffer, Protease Inhibitor (PI) Cocktail (Sigma Aldrich #P8340-1ML) was added at 6.5% of the final volume. Cultures were washed twice with cold DPBS to remove any dead cells. Cold lysis buffer (750 μ L) with 6.5% PI was added to each 10 cm² dish, 400 μ L per well in a 6-well plate. Cells were gathered using a clean rubber scraper and gently pipetted up and down 3 times. The cell lysate was transferred into a pre-chilled 1.7 mL centrifuge tube and kept on ice for 30 min. Samples were then centrifuged at 4°C for 16 min at 9500 x g. The supernatant was aliquoted into pre-chilled tubes and stored at -80°C.

Total protein in the samples was measured by using the BioRad DC protein assay kit (BioRad # 500-0016) as per the manufacturer's instructions. Serial dilutions of bovine serum albumin (BSA) were used as the protein standards (37.5 mg/mL to 0.58594 mg/mL). Absorbances of standards and cell lysates, each performed in duplicate, were

measured at 655 nm in a 96-well Model 680 Microplate Reader (Bio-Rad Laboratories). Using the Microplate Manager 5.2.1 Software (Bio-Rad Laboratories), protein concentrations of each sample was quantified based on standard curves derived from the BSA serial dilutions.

II. D. ii. mCLCA3 protein detection:

A rabbit anti-mCLCA3 specific polyclonal antibody corresponding to amino acids 252 to 267 (TEKNHNQEAPNDQNQR), conjugated to keyhole limpet hemocyanin (KLH) was synthesized (Invitrogen, Zymed Laboratories). This antibody was designated as AbMCLCA3 and was previously characterized and reported in analyzing mCLCA3 protein levels in mouse tissue [73]. AbMCLCA3 was used to specifically detect the N-terminal fragment of mCLCA3 that is approximately 75 kDa in size.

Cell lysates were prepared by adding 5X Laemmli buffer and denatured at 95°C for 3 min. Samples were chilled on ice, centrifuged and 50 µg of total protein was electrophoresed on a 10% SDS-acrylamide resolving gel at 100V for 2 hours. The separated proteins were then electrophoretically transferred onto PVDF Transfer Membranes (GE Healthcare #RPN303F) at 75V over 1.5 hours. Membranes were blocked for 1 hour at room temperature in block solution (1X PBS, 0.05% Tween-20 with 5% powdered skim milk) followed by incubation for 2 hours with the AbMCLCA3 (252-267) immune serum at a 1:2000 dilution. Membranes were rinsed once with PBS-T (1X PBS with 0.05% Tween-20) and washed six times for 6 min per wash. Membranes were then incubated with HRP-conjugated goat anti-rabbit (BioRad #170-6515) secondary antibody at a 1:200,000 dilution for 1 hour followed by washing with PBS-T as described

above. The blots were developed using the SuperSignal West Femto Kit Maximum Sensitivity Substrate (Pierce #34095).

II. D. iii. MUC3B protein detection:

Cell lysates were prepared as described above and electrophoresed on a 10% SDS acrylamide resolving gel at 100V for 2 hours. The separated proteins were then electrophoretically transferred onto PVDF Transfer Membranes at 75V over 1.5 hours. Membranes were blocked for 1 hour at room temperature in block solution followed by multiple washing in PBS-T and then incubation for 3 hours with Mucin3B(S-20) antibody (Santa Cruz Biotechnology #SC-102029) at a 1:300 dilution. Membranes were rinsed once with PBS-T and washed six times for 6 min per wash. Membranes were then incubated with HRP-conjugated goat anti-rabbit secondary antibody at a 1:100,000 dilution for 1 hour followed by washing with PBS-T as described above. The blots were developed using the SuperSignal West Femto Kit Maximum Sensitivity Substrate.

II. D. iv. β -actin normalization and densitometry quantification:

β -actin was used to ensure equal protein loading of each sample. Developed membranes were stripped by incubation with 100 mL of stripping solution (100 mM 2-mercaptoethanol, 2% SDS, 62.5 mM Tris-HCl, pH 6.7) for 30 min at 55°C. Membranes were then rinsed with TBS-T (1X TBS with 0.05% Tween-20) and washed with TBS-T for 7 min. Membranes were then washed with TBS twice for 5 min and blocked for 1 hour at room temperature in block solution. Stripped membranes were then re-probed with rabbit anti- β -actin (Santa Cruz Biotechnology #SC-1616) primary antibody at 1:8000 for 2 hours, rinsed once with PBS-T and washed six times for 6 min per wash.

Membranes were then incubated with HRP-conjugated goat anti-rabbit secondary antibody at a 1:20 000 dilution for 1 hour followed by washing with PBS-T as described above. The blots were developed using the SuperSignal West Femto Kit Maximum Sensitivity Substrate.

Protein bands of interest were scanned using the Fluorochem 8800 Image System (Alpha Innotech Corp.) and imported into the FluoroChem FC Standalone Program. Using the Spot Density Tool in the program, the density of each protein band of interest was measured. Any background present on the film was accounted for using the software's AUTO BACKGRD function. mCLCA3 and MUC3B band intensities for each sample, HT29, HT29-CaP, HT29trMCS and HT29trCLCA3 were normalized to the control β -actin bands.

II. D. v. Protein alignment using Blast-P search tool:

To align the AbMCLCA3 peptide sequence to other CLCA protein family members, Blast-P (NCBI) was used. The protein sequence of AbMCLCA3, TEKNHNQEAPNDQNNQ, was aligned to all human CLCA members, hCLCA1, hCLCA2, hCLCA3 and hCLCA4 to check for potential cross-reactivity of protein detection by western blot.

II. E. Histology

II. E. i. Cell culture on coverslips:

Cells were cultured onto glass coverslips in preparation for histological staining. The coverslips were first dipped into 70% isopropyl alcohol to prevent contamination and

were then washed thoroughly in pre-warmed, sterile PBS. Each coverslip was placed into the bottom of a 6-well plate with 2 mL of complete growth medium per well. Cells were seeded at 1:3 ratios and were allowed to grow until 18 days post-confluency.

II. E. ii. Alcian blue and nuclear fast red preparation:

To observe goblet vs. non-goblet cell formation in cell culture, two stains were used for all histological analysis. Alcian blue was used to stain goblet cells and nuclear fast red was used to stain non-mucus producing cells in culture. For alcian blue, 1 g of Alcian Blue 8GX (Sigma-Aldrich #A3157) was dissolved into 100 mL of 3% acetic acid. The 0.1% nuclear fast red stain was prepared by dissolving 5 g of aluminum sulphate (Sigma-Aldrich #368458-500G) into 100 mL of distilled H₂O and 0.1 g of Nuclear Fast Red (JT Baker #S635-01). The solution was slowly heated to a boil and was allowed to cool overnight. Both stains were filtered and as a preservative, thymol (Sigma-Aldrich #T0501-100G) was added to each dye.

II. E. iii. Fixing and staining of cells:

Cells were washed twice with pre-warmed DPBS to remove any residual medium. They were fixed with 3 mL of a fixative mixture, made of 1:3 glacial acetic acid to anhydrous methyl alcohol stored in -20°C, in 2 changes for 30 min each. During fixation, the plates were placed in -20°C. When the fixation steps were completed, the glass coverslips were removed from the 6-well plates and dried overnight at 60°C. The following day, each dried coverslip was stained in 2 mL of alcian blue dye for 20 min. The coverslip was washed in distilled H₂O and was counterstained in 2 mL of 0.1% nuclear fast red for 30 sec. The coverslip was washed again in distilled H₂O and was

mounted using a single drop of DPX on a glass slide. When the DPX was dry, the rim around each coverslip was sealed using nail-polish and each slide was appropriately labelled.

II. E. iv. Cell counts of stained cultures:

Brightfield digital images were taken of cell culture slides for comparison. Segmentation of images for goblet cell counting was done using the JMicroVision v1.27 software. Images taken at 10X magnification were processed for alcian blue stained goblet cells and empty goblet cells using Object Separation and Object Extraction features of the software.

II. F. Statistical analysis:

All values presented in graphs and figures are expressed as the mean \pm SEM. Student's T-tests (two tailed, unpaired) were performed to compare mRNA transcript levels, protein levels and goblet cell counts in mCLCA3 treated HT29 cultures with respect to untreated HT29, HT29-Cap and HT29trMCS cultures. Each 'n' value represents an independent treatment or transfection, treated in duplicate, for each experiment. qPCR comparing mRNA expression levels were performed in duplicate and normalized to endogenous β -actin mRNA levels. To evaluate protein expression levels, western blots were performed in duplicate and normalized to endogenous β -actin protein levels, and to evaluate goblet cell counts, histological staining was performed in quadruplicate. The results of each T-test gave a probability where if p was less than 0.05, there was a 95% chance that the results occurred non-randomly and the data was statistically significant. Any p value greater than 0.05 was considered non-significant.

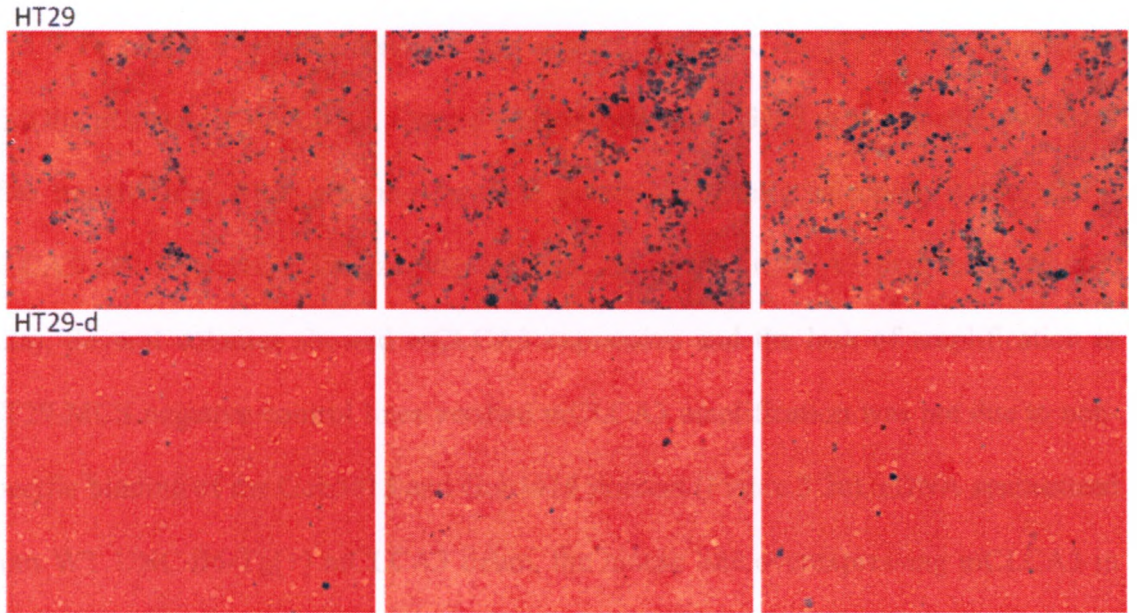
III. Results

III. A. Generation of differentiated HT29 cell lines (HT29-d)

HT29 cells were chemically induced into differentiation using NaBt as per Augeron and Laboisie [128]. Since this study concentrated on mCLCA3's effect on mucus and goblet cells, it was important to utilize a cell line with a sizeable goblet cell population much like HT29-Cl.19E. To determine the extent of goblet cell proportion to the total cell population in the butyrate treated cultures, HT29 and HT29-d cells were cultured 18 days past confluency, stained and analyzed as explained in section II. E. (Figure 3.1a). The population of alcian blue stained goblet cells in HT29 cultures (970 stained goblet cells per mm^2 , SEM= ± 64 , n= 6, 38 counts) were significantly higher than that of HT29-d cultures (56 stained goblet cells per mm^2 , SEM= ± 7 , n=6, 15 counts). On average goblet cell counts were over 15 times higher in HT29 cells compared to the chemically differentiated HT29-d cells (**p < 0.001) (Figure 3.1b).

Hundreds of clonal cell populations derived from chemically differentiated HT29 cultures were screened with results similar to the images shown in Figure 3.1a. Failure to obtain a cell line rich in goblet cells as the previously described HT29-Cl.19E cell line [128] meant that all experiments would be performed on the originally undifferentiated HT29 cells cultured 18 days past confluency. Differentiation of HT29 cells occurs when the cells are allowed to grow beyond confluency for an extended period of time. Findings published by Comolada *et al.* suggested 18 days post-confluency to be the ideal length of time for goblet cells to develop from undifferentiated HT29 cultures [130], making it an acceptable model for this study.

(a)



(b)

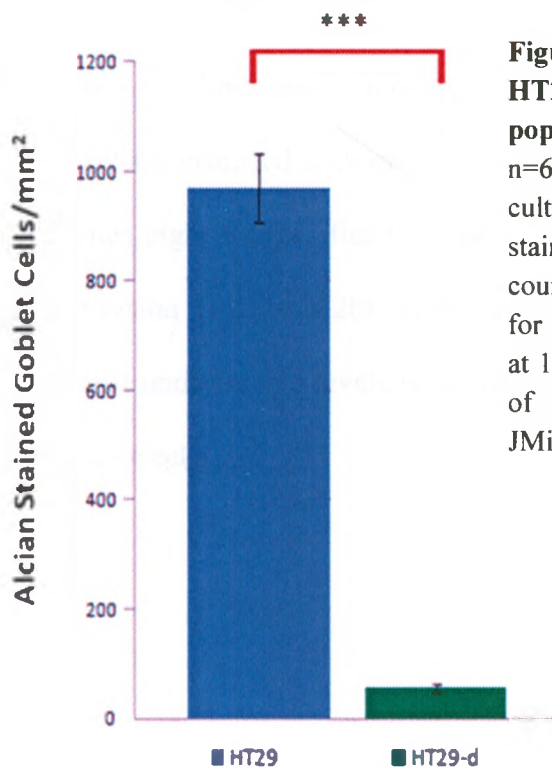


Figure 3.1. Histological stain of HT29 vs HT29-d cell cultures and goblet cell population analysis. (a) HT29 (top panel, n=6) and HT29-d (lower panel, n=6) cells cultured 18 days post-confluency, fixed and stained with alcian blue pH, 2.5 for 20 min, counterstained with 0.1% nuclear fast red for 30 sec. Brightfield digital images taken at 10X magnification. (b) Goblet cell counts of stained cultures performed using the JMicroVision v1.27 software. *** $p < 0.001$

III. B. Generation of stable HT29-CLCA3 cell lines

To obtain a cell line constitutively expressing mCLCA3, HT29 cells transfected with the pDream2.1-mCLCA3 plasmid were placed under G418 drug selection two days after transfection. After growing for four weeks under drug selection, stable HT29-CLCA3 cell lines were analyzed by RT-PCR to verify mCLCA3 expression (Figure 3.2a). Several colonies showed mCLCA3 expression and the lack of amplification in HT29-MCS negative control lines verified mCLCA3 amplification was not due to non-specific binding of the Gob5#15 and Gob5#16 primers (Figure 3.2c). cDNA synthesized from WT UNC·B6-Tg(+) mCLCA3 ileum, the mouse line overexpressing mCLCA3 in the intestine, was used as the positive control for this experiment.

All stable cell lines were maintained on G418 drug selection to maintain the population of cells transduced with mCLCA3. Total RNA collected from stable HT29-CLCA3 cell lines eight weeks after transfection were analyzed again by RT-PCR for mCLCA3 expression (Figure 3.2b). However, mCLCA3 expression was drastically reduced to almost undetectable levels when compared to the stable cultures under drug selection for four weeks.

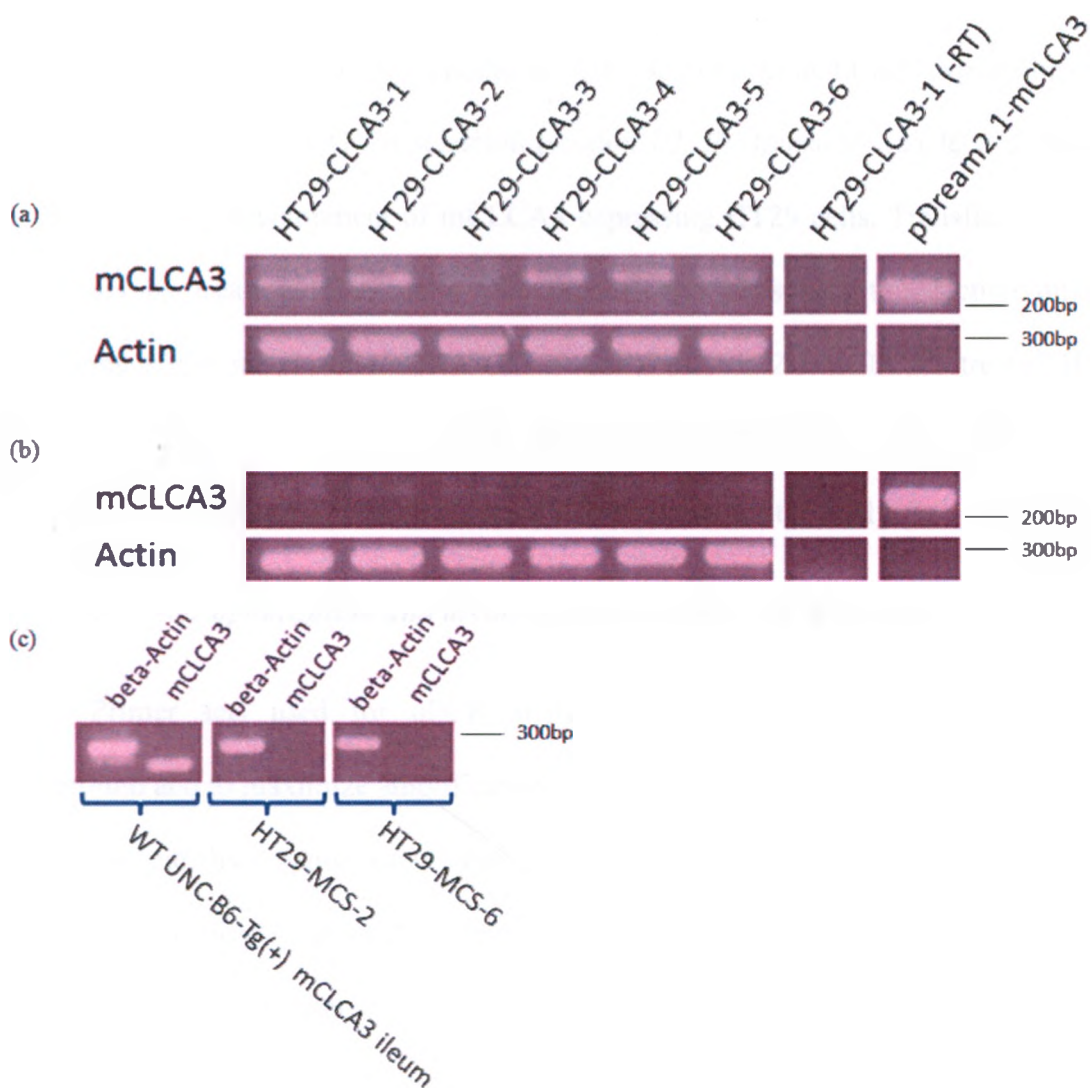


Figure 3.2. RT-PCR of stable transfected HT29-CLCA3 and HT29-MCS cell lines. (a) RT-PCR of stable cell lines transfected with pDream2.1-mCLCA3 and grown under G418 drug selection for four weeks, and (b) under G418 drug selection for eight weeks. (c) RT-PCR of stable cell lines mock transfected with empty pDream2.1-MCS vector under G418 selection. WT UNC-B6-Tg(+) mCLCA3 lane represents ileal cDNA obtained from transgenic WT B6 mouse overexpressing mCLCA3.

III. C. Generation of transient HT29-CLCA3 cell lines

To avoid the problems associated with decreased mCLCA3 expression over prolonged growth under G418 selection (section *III. B*), transient transfection became the focus for the development of mCLCA3 expressing HT29 cells. Transfections were performed by treating HT29 cells with the calcium phosphate transfection mixture containing either no plasmid/cDNA (HT29-CaP), pDream2.1-mCLCA3 treated HT29 cells (HT29trCLCA3) and the empty pDream2.1-MCS vector treated HT29 cells (HT29trMCS). Untreated HT29 cells were also prepared for the analysis.

III. C. i. Primer optimization and dissociation curves for qPCR analysis:

Primer sets used for qPCR analysis were optimized so as to minimize background and to maximize amplification of the desired gene product. Figures 3.3a and 3.3b show the dissociation curve and amplification plots of the primer set used for mCLCA3 detection. PCR product from the primers with 400 ng/ μ L of forward and reverse primer had the sharpest dissociation curve at 82°C (Figure 3.3a) and the highest amplification plot (Figure 3.3b). A single dissociation peak present in Figure 3.3a demonstrates that the primer set used for mCLCA3 detection has one single PCR product and there is no non-specific binding of the primers. Primer concentrations for MUC1, MUC2, MUC3B, MUC5AC, MUC5B and TFF3 were also selected based on these criteria and chosen concentrations are shown in Table 2.2.

cDNA samples were tested to verify no contamination by running standard curves with the MUC3B primer set. Dissociation curves of serial diluted cDNA samples and respective -RT controls were analysed. The dissociation curve of an HT29 cDNA

sample (Figure 3.3c) using MUC3B primers shows a single peak at about 83°C which confirms that the cDNA sample had no contamination. The dissociation curves of cDNA samples used for qPCR had to meet these conditions, and all samples used in these experiments met these criteria.

III. C. ii. mCLCA3 detection in transient cell cultures by RT-PCR and qPCR:

As an initial screen, RT-PCR was performed on HT29, HT29-CaP, HT29trMCS and HT29trCLCA3 cell lines to test amplification of mCLCA3. Only the HT29trCLCA3 cell cultures showed PCR product using the primers specific for mCLCA3 detection (Figure 3.4a, lane 7) and as expected, none of the -RT samples showed amplification product for either mCLCA3 or β -actin (Figure 3.4a, lanes 2,4,6,8).

Comparative quantification of HT29, HT29-CaP, HT29trMCS and HT29trCLCA3 lines verified the RT-PCR results (Figure 3.4b). After normalization to β -actin amplification levels, only HT29trCLCA3 cell cultures showed mCLCA3 amplification with an average fluorescence value of 7051 dRn (SEM= \pm 2126, n= 6). Untreated HT29 and the HT29-CaP, HT29trMCS controls showed no fluorescent counts of mCLCA3 amplification after 35 cycles.

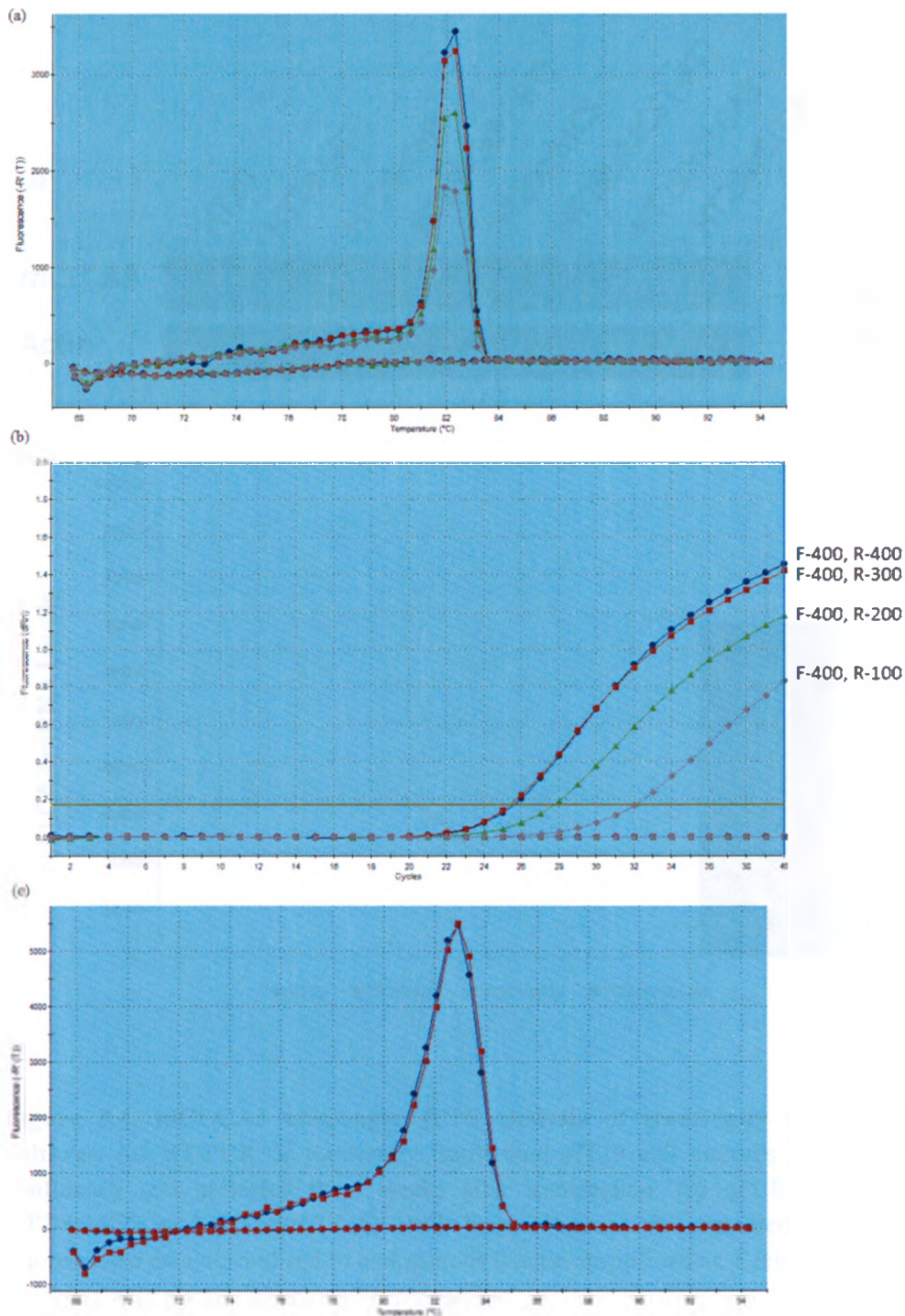


Figure 3.3. Dissociation curves and amplification plots for mCLCA3 primer set and HT29 sample. Primer optimization showing (a) dissociation curve and (b) amplification plot of mCLCA3 primer set performed at 95°C for 30 sec, 68°C for 1 min and 78°C for 30 sec over 35 cycles. F- indicates the concentration of the forward primer ($\mu\text{g}/\mu\text{L}$) and R- indicates the concentration of the reverse primer ($\mu\text{g}/\mu\text{L}$). (c) Dissociation curve of an HT29 cDNA sample using the MUC3B primer set.

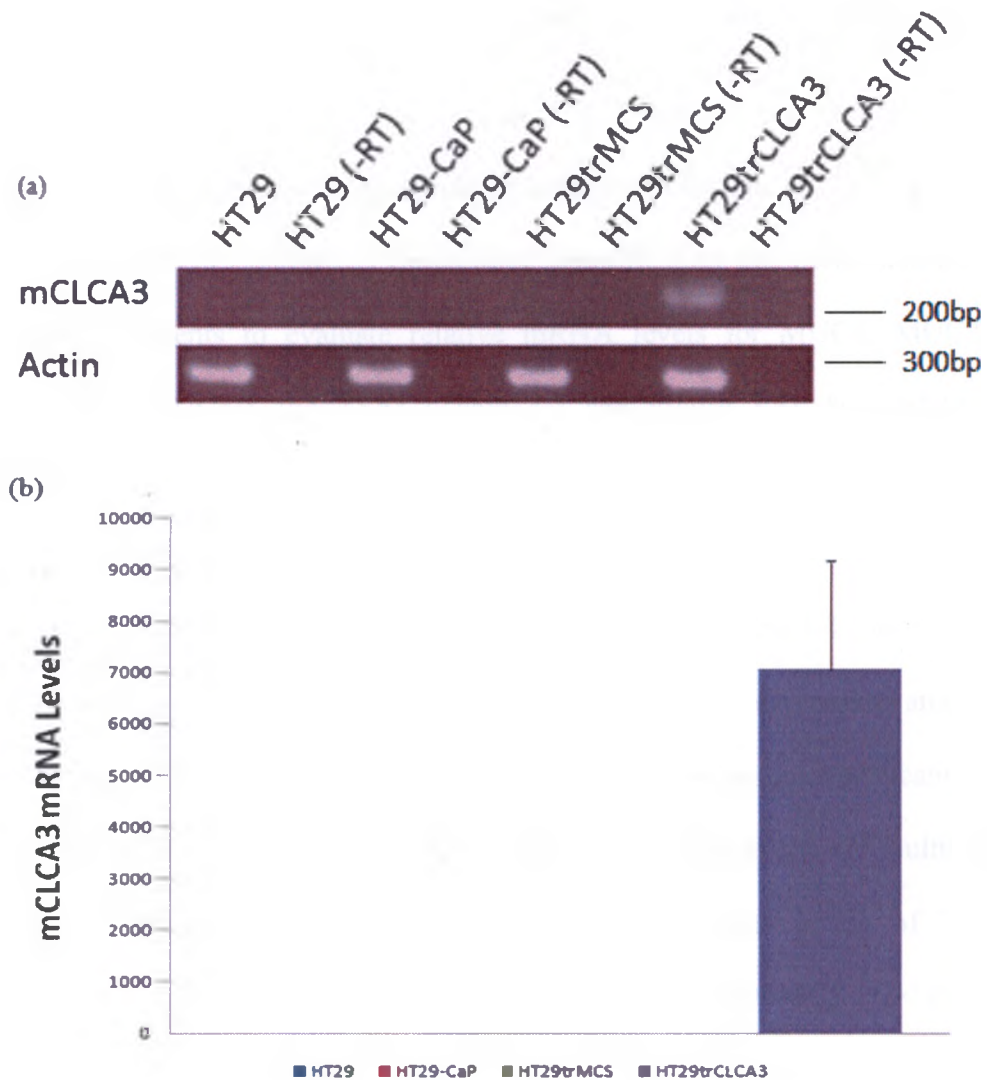


Figure 3.4. mCLCA3 messenger RNA analysis of transiently transfected HT29 cell cultures. (a) RT-PCR of transiently transfected HT29 cell cultures grown to 18 days past confluency and collected three weeks after transfection. (b) qPCR of HT29, HT29-CaP, HT29trMCS and HT29trCLCA3 cell lines. Values are presented as baseline-corrected fluorescence data normalized to endogenous β -actin amplification. Each sample was analyzed in duplicate with a total 'n' value of 6 per sample.

III. C. iii. mRNA analysis of the mucin family of genes and trefoil factor type 3:

As a potential modifier of mucus, HT29 cultures treated with mCLCA3 were analyzed for relative transcript levels of several mucins and of TFF3 to untreated and mock treated HT29 cultures. Comparative quantification was performed against all cell culture treatments to evaluate relative mRNA levels for MUC1, MUC2, MUC3B, MUC5AC, MUC5B and TFF3 (Table 3.2 and Figure 3.5). HT29trCLCA3 treated cultures had significantly lower levels of MUC1 transcripts compared to all other cell cultures (* $p < 0.05$) (Figure 3.5a). MUC2 mRNA levels were lower in the HT29trCLCA3 cultures compared to the HT29-CaP and the HT29trMCS lines (* $p < 0.05$), but there was no significant difference in MUC2 expression among untreated HT29 and HT29trCLCA3 cultures (Figure 3.5b). There was no significant difference in MUC3B, MUC5AC or MUC5B gene expression in any of the cell culture treatments (Figure 3.5c-e). HT29trCLCA3 cultures also had lower levels of TFF3 mRNA compared to untreated HT29 cells (** $p < 0.005$) and HT29trMCS (* $p < 0.05$), but there were no significant changes in TFF3 expression when comparing HT29trCLCA3 to HT29-CaP cultures (Figure 3.5f).

	HT29	HT29-CaP	HT29trMCS	HT29trCLCA3
MUC1	1 (± 0.174)	0.736 (± 0.101)	1.6 (± 0.319)	0.302 (± 0.018)
MUC2	1 (± 0.236)	0.989 (± 0.108)	5.931 (± 1.46)	0.575 (± 0.106)
MUC3B	1 (± 0.121)	0.638 (± 0.086)	0.198 (± 0.089)	0.529 (± 0.165)
MUC5AC	1 (± 0.113)	1.250 (± 0.111)	0.948 (± 0.301)	1.123 (± 0.293)
MUC5B	1 (± 0.114)	0.882 (± 0.110)	1.057 (± 0.336)	1.031 (± 0.282)
TFF3	1 (± 0.096)	0.668 (± 0.130)	1.142 (± 0.182)	0.511 (± 0.039)

Table 3.1. Relative MUC and TFF3 gene expression in untreated and treated HT29 cultures. qPCR analysis of relative expression levels of MUC1, -2, -3B, -5AC, -5B and TFF3 in HT29, HT29-CaP, HT29trMCS and HT29trCLCA3 cell lines. Fluorescence data from qPCR experiments normalized to endogenous β -actin amplification by the Stratagene Mx300P software. All values are presented relative to HT29 expression (\pm SEM), $n = 6$.

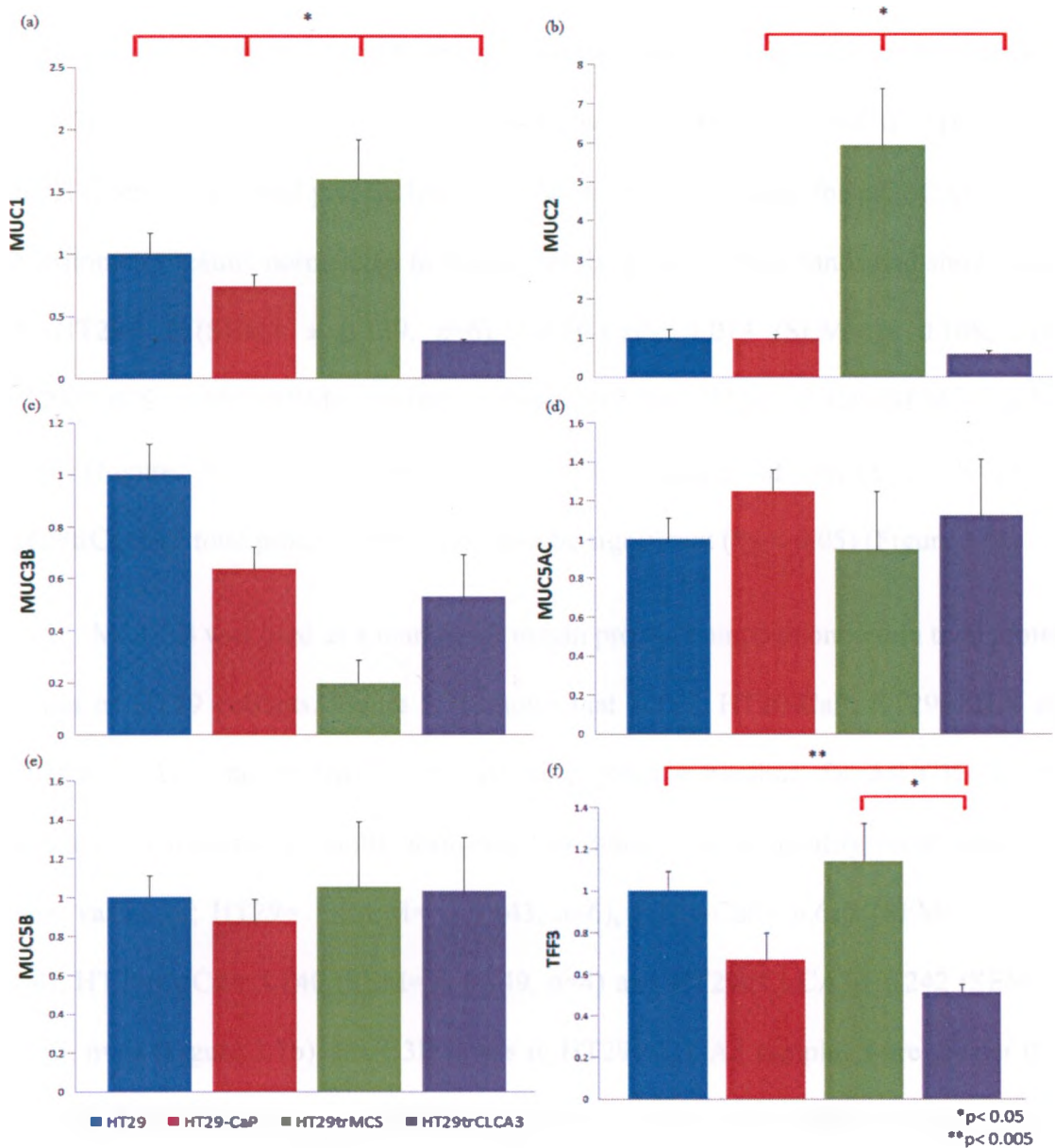


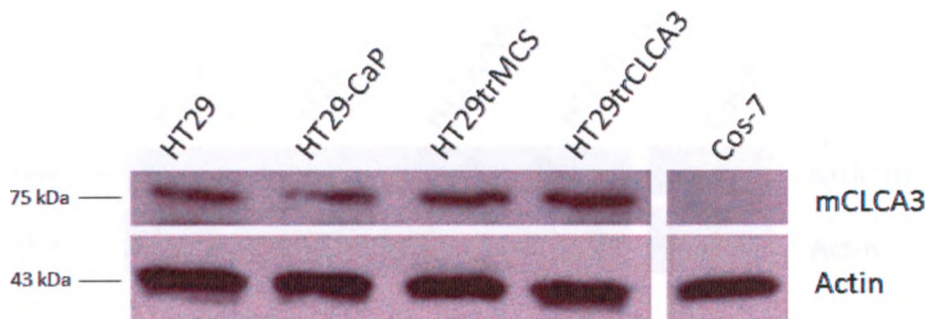
Figure 3.5. qPCR results of relative MUC and TFF3 mRNA levels. Comparative quantification was performed by qPCR experiments to compare relative mRNA transcript levels of (a) MUC1, (b) MUC2, (c) MUC3B, (d) MUC5AC, (e) MUC5B and (f) TFF3. All experimental results were normalized to endogenous β -actin amplification by the Stratagene Mx300P software. *p < 0.05, **p < 0.005, n=6 for all treatments.

III. C. iv. Protein analysis of mCLCA3 and MUC3B:

To verify that mCLCA3 transcripts within the HT29trCLCA3 cultures were being translated into full-length protein, western blot analysis was performed using AbMCLCA3 immune serum. Figure 3.6a shows that HT29, HT29-CaP, HT29trMCS and HT29trCLCA3 total protein lysates all have positive banding for mCLCA3 protein. Densitometry results normalized to β -actin levels quantify these bands and show values of: HT29= 1 (SEM= \pm 0.139, n=6), HT29-CaP= 1.014 (SEM= \pm 0.108, n=4), HT29trMCS= 1.087 (SEM= \pm 0.061, n=4) and HT29trCLCA3= 1.420 (SEM= \pm 0.086, n=6) (Figure 3.6b). The approximate 35% increase of mCLCA3 levels in HT29trCLCA3 total protein is shown to also be significant (*p < 0.05) (Figure 3.6b).

MUC3B was used as a marker for mucin protein composition within total protein lysates of HT29 cultures. Figure 3.7a shows that HT29, HT29-CaP, HT29trMCS and HT29trCLCA3 total protein lysates all have positive banding for MUC3B protein detection. Densitometry results normalized to β -actin levels quantify these bands and show values of; HT29= 1 (SEM= \pm 0.143, n=6), HT29-CaP= 0.617 (SEM= \pm 0.070, n=4), HT29trMCS= 1.140 (SEM= \pm 0.249, n=4) and HT29trCLCA3= 1.242 (SEM= \pm 0.155, n=6) (Figure 3.7b). MUC3B levels in HT29trCLCA3 samples were greater than HT29-CaP samples, about twice the amount of MUC3B was present in the mCLCA3 treated cultures (*p < 0.05). There was no significant difference among HT29, HT29trCLCA3 and the control HT29trMCS cultures.

(a)



(b)

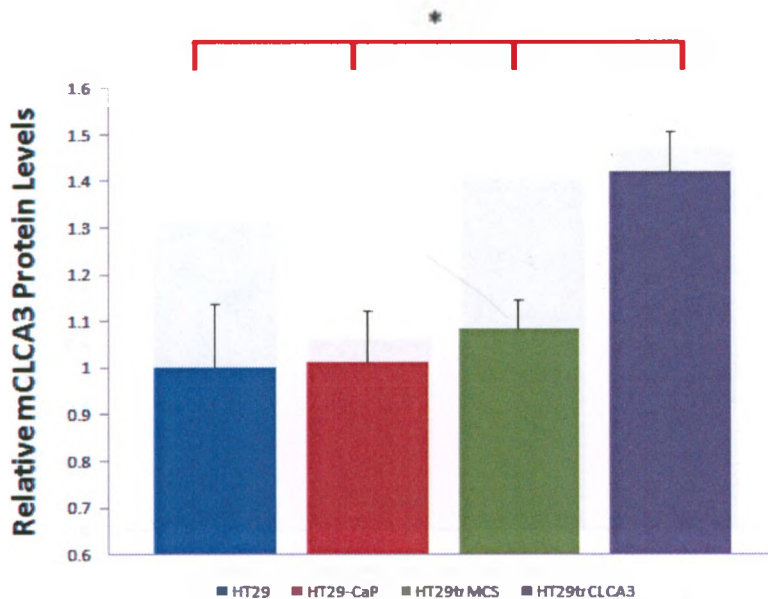
* $p < 0.05$

Figure 3.6. mCLCA3 western blot and densitometry results. (a) Total protein (50 μ g) was run on a 10% SDS-acrylamide gel and transferred to a PVDF membrane. Membranes were then incubated with either AbMCLCA3 immune serum (top panel) or β -actin primary antibody (lower panel). (b) Densitometry results were obtained using FluoroChem FC Standalone program. The band intensities were measured and then normalized to their respective β -actin bands. * $p < 0.05$, HT29 and HT29trCLCA3 had an $n=6$ and HT29-CaP and HT29trMCS had an $n=4$.

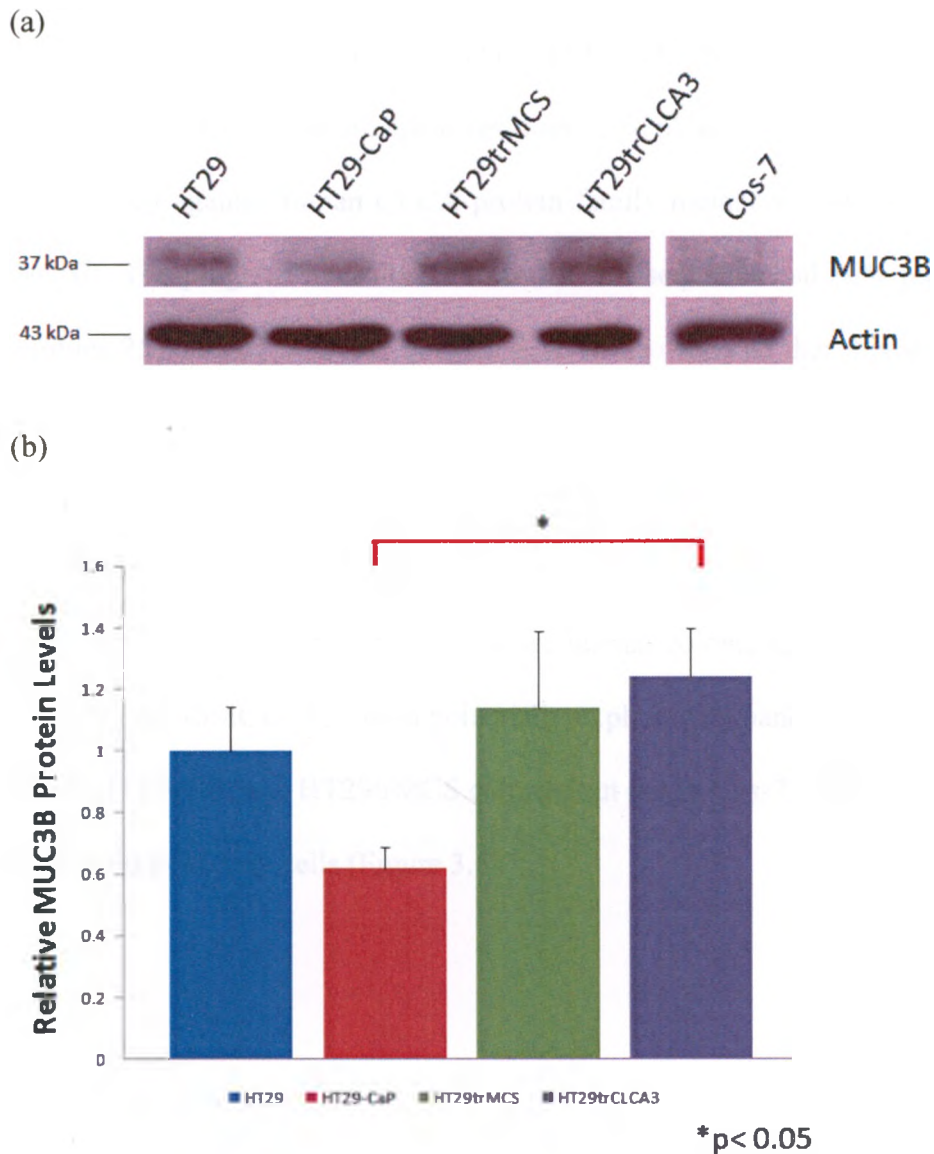


Figure 3.7. MUC3B western blot and densitometry results. (a) Total protein (50 μ g) was run on a 10% SDS-acrylamide gel and transferred to a PVDF membrane. Membranes were then incubated with either MUC3B (top panel) or β -actin primary antibodies (lower panel). (b) Densitometry results were obtained using FluoroChem FC Standalone program. The band intensities were measured and then normalized to their respective β -actin bands. * $p < 0.05$, HT29 and HT29trCLCA3 had an $n=6$ and HT29-CaP and HT29trMCS had an $n=4$.

III. C. v. BLAST analysis

The mCLCA3 peptide sequence TEKNHNQEAPNDQNNQ used to prepare the AbMCLCA3 immune serum spans residues 252-267 of the murine CLCA3 protein, and was aligned against human CLCA protein family members using the Blast-P program (NCBI). The program's results showed that this sequence had 80% positive identity to residues 251-265 of hCLCA1 (Figure 3.8). It also showed that this sequence had 67% positive identity to hCLCA4 from residues 251-265 (Figure 3.8). Sequence alignment of hCLCA2 and hCLCA3 showed 67% and 60% residue identity, respectively, to the CLCA3 antigen. hCLCA1 and hCLCA4 are the only CLCA members that are expressed in the human colon. Since HT29 cells are human colonic adenocarcinoma cells, cross-reactivity of AbMCLCA3 could potentially explain why bands are unexpectedly seen in HT29, HT29-CaP and HT29trMCS cultures but not in Cos-7 cultures, which are derived from monkey kidney cells (Figure 3.6b).



Figure 3.8. Sequence alignment of mCLCA3 antibody to human CLCA1 and -4. Using BLAST peptide sequence alignment, the CLCA3 antigen used to prepare the AbMCLCA3 antibody (corresponding to residues 252-267 of mCLCA3) used for western blots was compared against human hCLCA1 and hCLCA4 peptide sequences. 12 of 15 residues in hCLCA1 gave a positive sequence identification and 10 of 15 residues of hCLCA4 gave a positive sequence identification to the CLCA3 antigen. Residues in red indicate dissimilar amino acids affecting positive identification to the CLCA3 antigen. Green residues labelled with (+) indicate amino acids that differ in sequence but may have similar interactions to corresponding residues in the AbMCLCA3 peptide sequence.

III. C. vi. Histological Staining of cell cultures and goblet cell counts:

Histological staining of each cell culture was performed as described in section II. E. In contrast to the alcian blue stained cells that stain an intense blue due to the heavily glycosylated mucins within goblet cells, there were noticeable occurrences of cells that remained relatively unstained by the alcian blue or nuclear fast red dyes. These cells (Figure 3.9a, green arrow) shared similar size, shape and most importantly they shared very similar clustering throughout the culture as the alcian stained goblet cells seen in HT29 stains. These cells were designated as “empty” goblet cells due to the occasional faint staining by the alcian blue dye in some of these cells and their shared appearance to the alcian blue stained cells (Figure 3.9b, lower right-hand corner of right panel). Mucin degranulation, the ultimate purpose of goblet cells in the epithelial layer, would explain the presence of these “empty” goblet cells that do not stain the intense blue after exposure to the alcian blue dye. The theca, devoid of mucus leaving a very large volume of the cell empty, would be responsible for the faint-pink colouration as the nuclear fast red dye stains these goblet cells less intensely due to the proportional lack of organelles of goblet cells compared to other epithelial cells.

Using the JMicroVision v1.27 software, goblet cell counts were obtained for each cell line. The number of alcian blue stained goblet cells per mm^2 for each cell line is presented in Table 3.2 and Figure 3.10a, along with the number of empty goblet cells per mm^2 . HT29trCLCA3 cultures had significantly less alcian blue stained goblets compared to untreated HT29 cell cultures (* $p < 0.05$) but the mCLCA3 treated cultures had a considerably larger population of alcian blue stained goblet cells compared to the HT29-CaP and HT29trMCS negative control cultures (** $p < 0.001$) (Figure 3.10a,

Table 3.2). The number of empty goblet cells in the HT29trCLCA3 cultures was significantly lower than all other cell cultures (***) $p < 0.001$).

	HT29	HT29-CaP	HT29trMCS	HT29trCLCA3
Stained	969 (± 64)	143 (± 10)	128 (± 14)	805 (± 41)
Empty	738 (± 15)	1305 (± 23)	712 (± 18)	438 (± 15)
TOTAL	1707 (± 41)	1448 (± 60)	840 (± 36)	1243 (± 29)

Table 3.2. Goblet cell counts in untreated and treated HT29 cell cultures. Cell counts for alcian blue stained and empty goblet cells were performed using the JMicroVision v1.27 software. There were 38 counts made for alcian-blue stained goblet cells in HT29 cultures ($n=6$), 71 counts in HT29-CaP ($n=6$), 61 counts in HT29trMCS ($n=6$) and 67 counts in HT29trCLCA3 cultures ($n=6$). There were 34 counts made for empty goblet cells in HT29 cultures ($n=6$), 51 counts in HT29-CaP ($n=6$), 42 counts in HT29trMCS ($n=6$) and 68 counts in HT29trCLCA3 cultures ($n=6$). Data presented as number of goblet cells counted per mm^2 (\pm SEM).

Positive staining with alcian blue occurred in: 56.8% of the 1707 total goblet cells in HT29 cultures, 9.9% of the 1448 total goblets in HT29-CaP cultures, 15.2% of the 840 total goblets in HT29trMCS cultures and 64.8% of the 1243 total goblets in HT29trCLCA3 cultures (Figure 3.10b). Although there is a significantly lower total number of goblets in HT29trCLCA3 cultures than in HT29 (***) $p < 0.001$) and HT29-CaP (* $p < 0.05$), it is evident that a higher percentage of goblet cells retain their mucus in mCLCA3 treated cultures compared to the mock transfections (Figure 3.10b).

With respect to the total cell population, Figure 3.10c shows that 20.0% of stained HT29 cells were goblet cells and 11.3% of the total cell population were alcian blue stained goblets. For the HT29-CaP cultures, 18.7% of the cell population was made

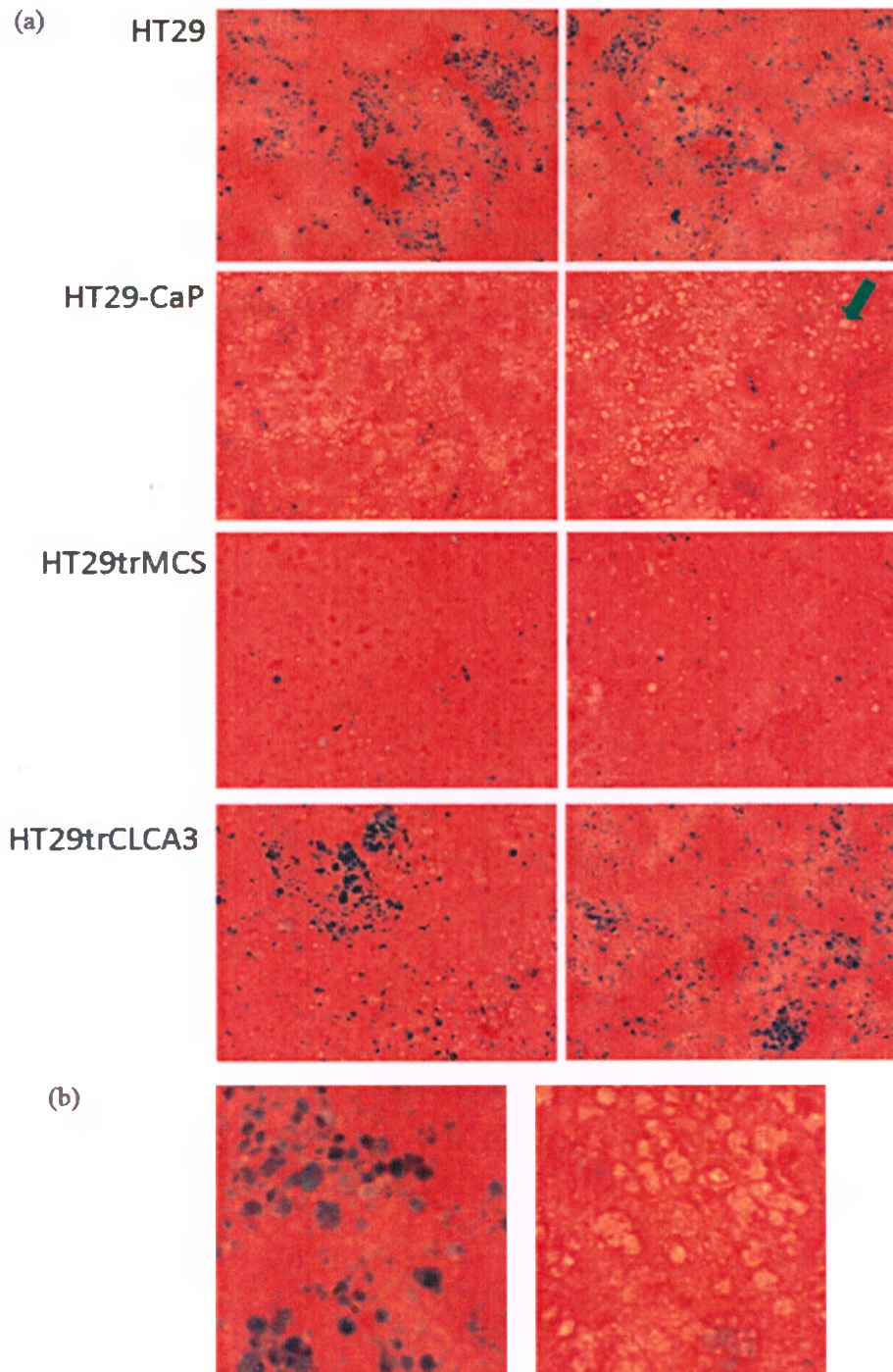


Figure 3.9. Histological stain of untreated HT29 and treated HT29 cell cultures. (a) Untreated HT29 cells and treated cells (HT29-CaP, HT29trMCS, HT29trCLCA3) were cultured to 18 days post-confluency before being fixed, stained with alcian blue pH 2.5 for 20 min and counterstained with 0.1% nuclear fast red for 30 sec. Brightfield digital images taken at 10X magnification. (b) Close up photos of mucus-filled HT29trCLCA3 (left, blue cells) and empty HT29-CaP (right, faint-pink cells) goblet cells.

up of goblet cells with 1.8% of the total cell population being mucus-filled goblets (Figure 3.10c). Only 10.8% of the HT29trMCS cell population was composed of goblet cells and only 1.6% were alcian blue stained goblets (Figure 3.10c). 16.8% of HT29trCLCA3 cell cultures were made up of goblet cells and 10.9% of the total cell population was composed of alcian blue stained goblet cells (Figure 3.10c).

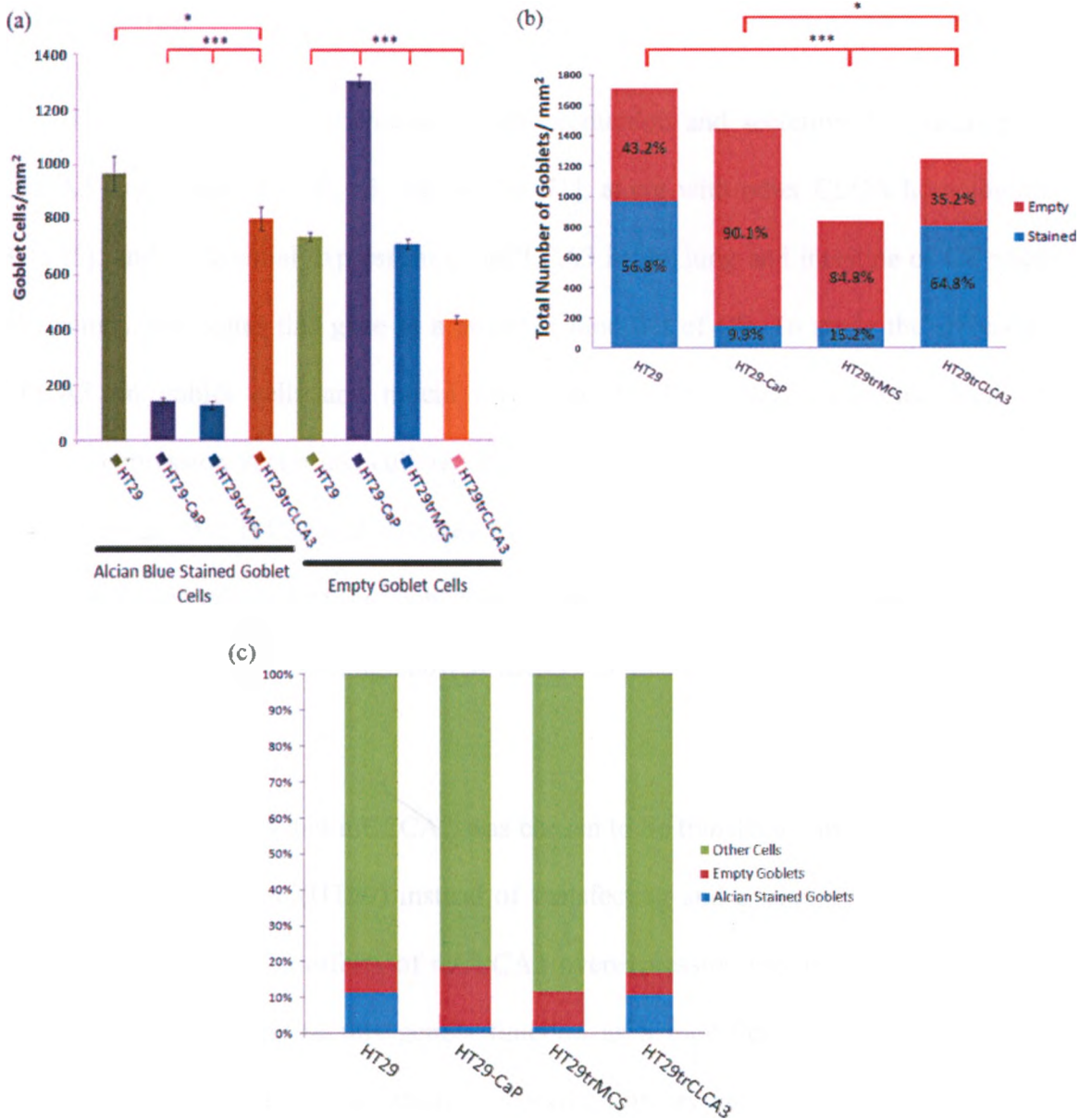


Figure 3.10. Goblet cell population analysis of cell culture stains. (a) Stained cell culture images for HT29 cells and each treatment of HT29 cells were used to obtain and compare goblet cell counts. Goblet cell counts were performed using the JMicroVision v1.27 software. (b) Total number of goblet cells compiled for HT29, HT29-CaP, HT29trMCS and HT29trCLCA3 stained cultures (all treatments had an n=6). Percentages of total goblet cell populations are shown for stained and unstained goblets. (c) Graph showing the percentages of alcian blue stained and empty goblet cells with respect to the total cell population. * $p < 0.05$, *** $p < 0.001$.

IV. Discussion

The observations of increased mucus production and secretion associated with mCLCA3 expression [59, 60, 63, 64, 68, 70, 71], along with other CLCA homologues [131-135], and differential expression of mCLCA3 in the lung and intestine of CF mice [43] strongly implicates this gene as a potential modifier of CF. To study the effects of mCLCA3 on goblet cells and mucin levels, HT29 cells were transfected with an mCLCA3 expression vector and cultured to 18 days post-confluency. The results of these studies showed that HT29 cell cultures transiently transfected with mCLCA3 had a higher percentage of mucus-filled goblet cells compared to the mock transfected control cultures and histological staining showed mCLCA3 treated cultures closely resembled untreated HT29 cultures.

There are reasons that mCLCA3 was chosen to be transfected in a human colonic adenocarcinomic cell line (HT29) instead of transfecting and overexpressing its human orthologue, hCLCA1. The effects of mCLCA3 overexpression observed in a transgenic mouse model of CF proved this gene's function as a modifier of the CF phenotype observed in mice [73]. From this study, a working primary antibody was available that had been characterized for detection against the N-terminal fragment of the mCLCA3 protein [73]. At the inception of this work, it was not known if this antibody specifically designed against mCLCA3 would also detect hCLCA1. Since mCLCA3 and hCLCA1 are orthologs, they are believed to have similar functions and be similarly processed in mouse and human tissues. Thus the original intent was that expressing mCLCA3 in human cells would yield a product that closely resembled endogenous hCLCA1 and mimic its function in these cells. In turn, the development of a system to allow for

mCLCA3 expression in HT29 cells would allow analysis of its effects on the production, processing and/or secretion of mucus/mucins and whether it would affect HT29 cell differentiation and goblet cell development.

IV. A. Generation of chemically differentiated HT29 cells

In order to study the role of CLCA in cell differentiation and the development of goblet cells, we followed an original protocol from a paper published by Augeron and Laboisse [128], who used 5 mM sodium butyrate on HT29 cell cultures. This chemical-mediated differentiation resulted in a cell line, called HT29-C1.19.E, with corresponding high numbers of goblet cells being developed over time in culture [128]. Unfortunately this experimental approach was unsuccessful in establishing a cell line rich in goblet cells. Staining of the chemically modified HT29-d cells with alcian blue, which is an ideal dye for acidic glycoproteins like the mucins present in the GI tract, did not result in enhanced staining.

Of the hundreds of isolated HT29-d colonies that were tested, none had a high percentage of goblet cells (section *III. A*). It is possible that there was a low goblet cell population in each HT29-d colony due to isolation of multiple colonies in close proximity, leading to a heterogeneous mixture of cell types and a “dilution” of goblet cells with respect to the total cell population. This explanation is very unlikely since steps were taken to ensure isolation of single colonies with the use of cloning rings and inspection under microscope. Prolonged exposure of cell cultures to butyrate also had no change in goblet cell counts, suggesting that the butyrate treatment lead to complete differentiation of all surviving cells in culture. The most likely explanation for a lack of

goblet cells in HT29-d cultures is that resultant cell colonies, originating from a small handful of founder cells, had a heterogeneous make-up with a very low ratio of goblet cells before being passed to larger wells and screened by histological stains. The results of this butyrate treatment and those published by Augeron and Laboisse [128] suggest that differentiation of HT29 cultures into the HT29-C1.19E line is a rare occurrence.

Butyrate is a short-chain fatty acid that is a by-product of dietary fiber fermentation by colonic bacterial flora [136] and is considered as the major energy substrate for colonocytes [137]. Butyrate clearly has a significant role in cellular growth as it can induce inhibition of histone phosphorylation [138], thus impairing cell growth mainly in the G1 phase of the cell cycle [139], and it has a role in mucosal repair during conditions that cause inflammation of the gut [140, 141]. Butyrate also induces differentiation and apoptosis in actively proliferating HT29 cells [130]. The induction of HT29 differentiation/apoptosis by chemical means was observed as proliferation of cell cultures were drastically reduced by increasing the concentrations of butyrate and other short-chain fatty acids normally present in the colon [130]. Moreover, it was shown that butyrate had no effect on already differentiated cells as surviving butyrate-treated cells proliferated without difficulty under prolonged butyrate treatments [130].

When untreated HT29 cells reach confluency they develop a polarized epithelial phenotype, forming contacts to neighbouring cells and undergo differentiation very similar to how a normal epithelial layer would develop in the colon [142]. Since HT29 cells were shown to have more goblet cells per mm^2 than the butyrate treated HT29-d cells, all subsequent experiments were performed on untreated HT29 cell cultures. These untreated cells underwent differentiation after reaching confluency and were maintained

in complete growth medium for another 18 days as per [130]. Repeated staining experiments of untreated HT29 cells grown 18 days post-confluency gave consistent results and was considered as a suitable and reliable method of obtaining adequate goblet cell levels (sections *III. A* and *III. C. vi*).

IV. B. Stable expression of mCLCA3 in HT29 cultures

The intent of stably expressing mCLCA3 in HT29 cultures was to establish a relevant model for studying the effects of mCLCA3 on goblet cell development, mucin production and mucus secretion. Several transfected cell lines cultured under G418 selection showed promise as RT-PCR results demonstrated mCLCA3 expression 4 weeks after transfection (section *III. B*). Unfortunately, analysis of these same cell cultures 8 weeks after transfection by RT-PCR showed that mCLCA3 expression levels to be severely reduced in comparison to the cells collected 4 weeks after transfection. Since analysis of β -actin was performed at the same time, and levels of this control remained consistent in these cultures, this suggests something had specifically affected mCLCA3 expression in these cells.

Since all stable cultures were grown under G418 selection, it can be safe to assume that all surviving cells are expressing the neomycin gene on the pDream2.1-mCLCA3 plasmid (or the pDream2.1-MCS vector in the control cells transfected with the empty vector). The inability to establish HT29 cell lines stably expressing mCLCA3 may be due to the CMV promoter responsible for the transgenic expression. The CMV promoter is a very common promoter used in eukaryotic cell expression when establishing stable cell lines, but experiments studying the CMV promoter's effectiveness

have shown that silencing can be a problem when using the CMV promoter in various cell types [143, 144]. A study performed on the human colonic HT29 cell line also showed silencing of the CMV promoter, leading to heterogeneous transgene expression throughout the cell population [145]. As early as 2-3 weeks after transfection, HT29 clones were expressing the transgene but silencing of the CMV promoter was observed in about 60% of the cell population [145].

The RT-PCR results taken at 4- and 8-weeks after transfection strongly suggest that silencing of the CMV promoter has taken place. As the efficiency of the CMV promoter has been shown to deteriorate as early as 3 weeks after transfection specifically in HT29 cells [145], silencing of the CMV promoter 8 weeks after transfection is the most likely scenario that would explain a lack of mCLCA3 expression in the stably transfected HT29-CLCA3 lines. These results also suggest the possibility that mCLCA3 overexpression in HT29 cultures may cause toxicity, potentially leading to the induction of transgene silencing as a survival mechanism. Alternate protocols for the expression of mCLCA3 were therefore required to assess its effect on HT29 cultures.

IV. C. Transient expression of mCLCA3 in HT29 cultures

With failure to establish a stable HT29 cell line expressing mCLCA3, subsequent experiments were performed on HT29 cell cultures that were transiently transfected with the pDream2.1-mCLCA3 plasmid. Transfected cells reached confluency approximately 2-3 days after treatment and were maintained for 18 days post-confluency to allow for proper differentiation of cultures. At this point, total RNA and protein collection, and cell staining were performed (approximately 21 days after transfection). The murine CLCA3

gene expression in the HT29trCLCA3 cell line was verified by RT-PCR and further confirmed by qPCR, with an expected lack of expression in all other cell cultures (section *III. C. ii*).

Detecting mCLCA3 protein using the AbMCLCA3 antibody yielded unexpected results as the lysates of all cell cultures, HT29, HT29-CaP, HT29trMCS and HT29trCLCA3, contained an immunoreactive band at the expected 75 kDa size (section *III. C. iv*). There are two possible explanations for these results; either the AbMCLCA3 antibody caused non-specific banding that develops at 75 kDa or AbMCLCA3 might be able to detect human CLCA proteins. BLAST analyses showed that the sequence of the AbMCLCA3 antibody matched up with hCLCA1 (80% positive sequence identity) and to a lesser extent hCLCA4 (67% positive sequence identity) from residues 251 through 265 (section *III. C. v*). The potential of cross-reactivity using this antibody is quite possible as both hCLCA1 and hCLCA4 are expressed in the human colon and thus likely expressed in HT29 cells [41, 53, 146]. There is also potential of AbMCLCA3 cross-reactivity to hCLCA2 (67% positive sequence identity by BLAST analysis) and hCLCA3 proteins (60% positive sequence identity by BLAST analysis). The chances of detecting these proteins are less likely since neither hCLCA2 or -3 are significantly expressed in the colon [146]. The AbMCLCA3 antibody was initially produced for the intended analysis of mouse tissue and so the potential for cross-reactivity to human homologues of mCLCA3 was not considered at the time. Processing of hCLCA proteins and mCLCA3 are also thought to be very similar which would potentially yield similar sized N-terminal target products (approximately 75 kDa).

By western blot analysis using the AbMCLCA3 antibody, there was an approximate 35% increase of CLCA protein detected in HT29trCLCA3 cultures, which suggests that the increase is most likely a result of mCLCA3 expression (section III. C. iv). Although it remains possible that bands observed at 75 kDa are due to non-specific binding of the AbMCLCA3 antibody, there was no band observed in Cos-7 samples, a cell line derived from the African green monkey kidney. These results suggest that AbMCLCA3 likely detects hCLCA1 protein in HT29 cultures in addition to mCLCA3 protein detection. Most importantly, the significant increase of mCLCA3 protein seen in HT29trCLCA3 cultures means any resultant changes observed in comparison to the other cultures can be attributed to mCLCA3 overexpression.

IV. C. i. Effect of transient mCLCA3 expression on MUC and TFF3 transcripts

Expression of mCLCA3 in HT29 cells shows a significant decrease in the mRNA transcript levels of MUC1. This suggests that mCLCA3 may have an effect on down-regulating MUC1 gene expression in the HT29 colonic cell line. If the effects of mCLCA3 on MUC1 transcription are indicative of the potential down-regulation on translational levels, this could have enormous implications as MUC1: is expressed in all secretory epithelial cells [100]; can be 'shed' from the cell surface by proteolytic cleavage, potentially being a significant contributor to the composition of mucus secretions [147, 148]; and is also a marker of cancer as MUC1 overexpression appears in many types of carcinomas including breast, lung, colon and pancreas [107, 149]. If mCLCA3 can have an effect on the levels of MUC1 protein in the colon (and potentially other tissues), it is quite likely that hCLCA1 would have a similar effect on MUC1. This means it has the potential to improve mucus composition and favour a less dense mucus.

This may also help to explain the ameliorative properties of CLCA seen in the luminal intestinal mucus of CF transgenic mice [73]. Down-regulation of MUC1 by mCLCA3, and potentially hCLCA1, could also help to modulate the proliferation of cancerous cells in various tissues. Of course, more in depth analysis is required to test these hypotheses of mCLCA3/hCLCA1 expression on the down-regulation of MUC1.

MUC2 gene expression was lower in HT29trCLCA3 cultures only when compared to HT29-CaP and HT29trMCS cultures, but there was no significant difference in MUC2 transcript levels among untreated HT29 and HT29trCLCA3 cultures. The abnormally high levels of MUC2 mRNA in the HT29trMCS line may be due to a significantly lower number of goblet cells present (average of only 10.8% of cells in culture were goblet cells compared to over 16% average in other cultures) that are forced to compensate for MUC2 secretion by overexpressing the gene. These inconsistent results cannot confirm whether mCLCA3 can regulate the transcription of the MUC2 gene in HT29 cells and it still remains possible that MUC2 gene expression can be regulated by mCLCA3 in the small intestine.

HT29trCLCA3 cultures had no significant effect in MUC3B, MUC5AC and MUC5B expression levels when compared to the other treated HT29 cells in culture. This could possibly be explained by each gene's expression profile, as MUC3 is predominantly expressed in the small intestine and MUC5AC and MUC5B are the major mucins expressed in the lung. These results suggest that regulation of MUC3, MUC5AC and MUC5B in HT29 cells is likely unaffected by mCLCA3. mCLCA3 could have an effect on the expression of these mucins if studied in appropriate cell lines derived from

the lung (for MUC5AC, MUC5B) and small intestine (for MUC3B) where these genes are normally expressed at higher levels.

HT29trCLCA3 cultures also had lower levels of TFF3 transcripts than untreated HT29 and HT29trMCS cultures, but had no significant difference to HT29-CaP treated cells. Since TFF3 signalling peptides have been shown to co-localize with secreted MUC2 protein [126], changes in TFF3 mRNA levels should correspond to similar changes in MUC2 mRNA levels. Unfortunately this presumption can only be supported when comparing HT29trMCS and HT29trCLCA3 cultures, where decreased TFF3 transcripts correlates to decreased MUC2 mRNA levels. These results do not support any modifying effect caused by mCLCA3 on MUC2, -3B, -5AC, -5B or TFF3 gene expression. These experiments that study the mRNA transcript levels need to be paired with corresponding studies at the protein level in order to obtain a clearer picture of the potential role mCLCA3 may have in the regulation of mucins and TFF3 peptide in HT29 cultures.

IV. C. ii. Effect of transient mCLCA3 expression on MUC3B protein

As a marker for mucin composition of HT29 mucus, MUC3B protein levels were tested by western blot analysis. Densitometry analysis shows that the levels of MUC3B protein were higher in cultures expressing mCLCA3 when compared to HT29-CaP cultures, but there was no difference in MUC3B levels among HT29, HT29trMCS and HT29trCLCA3 cultures (section *III. C. iv*). Since mRNA studies showed no significant difference in MUC3B levels, these results suggest that the regulation of MUC3B protein could be affected at the post-transcriptional and/or translational level. The changes in

MUC3B protein levels suggest that the regulation of synthesis is likely not attributed to mCLCA3 expression because there is no observable change in the protein levels of untreated HT29, HT29trMCS and HT29trCLCA3 cultures.

HT29 and HT29trCLCA3 cultures have a much higher percentage of mucus-filled goblet cells than the HT29-CaP and HT29trMCS controls, an approximate 5.5:1 ratio. It would therefore be expected that MUC3B protein levels would be significantly higher in HT29 and HT29trCLCA3 cultures but this was not the case. These results indicate that it is very likely MUC3B is not a major contributor to the colonic mucus of HT29 cells.

As discussed previously, protein studies on the remaining mucins and TFF3 will help to establish a clearer picture on mCLCA3's role in HT29 cells. Analyzing mucin protein levels can be difficult as mucin antibodies can behave unpredictably due to differential mucin processing. Antibodies made against specific sequences within the tandemly repeating serine/threonine-rich regions can become useless when these regions become heavily glycosylated after processing [150]. Fortunately, more commercially produced antibodies are becoming available for each mucin type which should hopefully make protein study less difficult in the near future.

IV. C. iii. Effect of transient mCLCA3 on goblet cell morphometry

Histological staining shows that transient mCLCA3 expression likely promotes mucus retention in HT29 cells. Untreated HT29 had the highest percentage of goblet cells with an average of 20% of the total cell population composed of goblet cells (section III. C. vi.). HT29-CaP and HT29trCLCA3 cultures followed closely behind with goblet cell averages of 18.7% and 16.8% of the total cell population, respectively, while

HT29trMCS cultures had a 10.8% goblet cell average (section *III. C. vi.*). The significantly lower average in HT29trMCS cultures is an unexpected result as it was supposed to resemble the total goblet cell population of HT29-CaP cultures.

Under normal growth conditions, just over half of HT29 goblet cells retain their mucus. The remaining goblet cells would await any triggers or insults before undergoing mucin degranulation. Untreated HT29 cultures represent the normal model of goblet cell morphometry for an intestinal epithelial layer, as these cells were not subjected to any levels of stress or injury (described below) in comparison to the other treatments of HT29 cells.

The percentage of goblet cells in HT29-CaP and HT29trMCS cultures are significantly different, but they share an important property where the goblet cell population is predominantly empty goblets (90.1% for HT29-CaP and 84.8% for HT29trMCS). Excessive mucin degranulation could be a result of exposure to severe growth conditions, namely the transfection protocol. Transient transfection was performed using calcium-phosphate precipitation and all buffers used for transfection were both sterile and at a neutral pH to help prevent cell toxicity. Although this common method of transfection can be very effective, the major problem of calcium-phosphate coprecipitation with DNA is the potential drop in pH that occurs during transfection, causing acidification of the medium and cell death [151]. Residual salts present on the walls of the culture dishes following transfection may have altered the pH of growth medium and contributed to harsher than normal conditions over 18 days. This could be an explanation for such a high percentage of empty goblet cells in HT29-CaP and HT29trMCS cultures as this change in the cellular environment could emulate potential

stresses or insults experienced by the intestinal epithelium, and the natural response would be collective mucus secretion as the goblet cells naturally attempt to protect the epithelial layer.

HT29 cultures transiently expressing mCLCA3 did not exhibit goblet cell hyperplasia, a phenomenon indicative of mCLCA3 overexpression in the mouse intestine [73]. Goblet cell metaplasia, on the other hand, has been well established in many studies of mCLCA3 overexpression in the mouse lung [152, 153]. It would be difficult to predict goblet cell metaplasia in HT29trCLCA3 cultures, as transfection of the mCLCA3 gene occurs as the cells are developing a confluent layer and therefore still not fully differentiated. Total goblet cell numbers of HT29trCLCA3 cultures are actually lower than both untreated HT29 and HT29-CaP cultures. Because goblet cell hyperplasia was not observed in HT29trCLCA3 cultures, these results suggest that mCLCA3 does not directly induce non-differentiated HT29 cells to become goblet cells as an epithelial monolayer forms.

Despite the potentially harsh transfection conditions, the most compelling argument that can be made from the analysis of goblet cell morphometry is that mCLCA3, and potentially hCLCA1, acts to either (a) induce mucin production in order to replenish goblet cells with newly synthesized mucin granules following mucin degranulation or (b) promote mucus retention within goblet cells. This is supported by the observation that almost 65% of HT29trCLCA3 goblet cells are mucus-filled. While both functions would explain the high percentage of goblet cells containing mucus, the consequences of each pathway would lead to different mucous properties at the epithelial layer.

If mCLCA3 has a direct role in stimulating the production of select mucins to replenish depleted goblet cells, it would not only support mCLCA3's role as a modulatory factor of mucus, but it would also significantly alter mucosal rheology by accelerating mucus release. This would lead to a larger intestinal mucus volume, providing a larger network for which substrates must transverse in order to interact with the epithelial layer. Histological staining showed some goblet cells with varied intensities of alcian blue staining, which could be a result of an intermediary state of mucus replenishment in goblet cells. Analysis of cultures transiently expressing mCLCA3 that have reached confluency beyond 18 days could establish whether intensity of alcian blue staining increases among the goblet cell population, but this comes with the risk of decreased mCLCA3 expression potentially due to promoter silencing over time (as described in section *IV. B.*)

If mCLCA3 instead can promote mucus retention, it would significantly support its role as a modulatory factor of the mucosal layer in the intestinal epithelium. In this situation mCLCA3 would act to limit the mass/volume of mucus possibly through an inhibitory interaction with MARCKS, which is protein responsible for mucin degranulation [90]. Studies have shown that mCLCA3 has a significant role in mucin upregulation [68, 135], but previous work in this lab has also shown mCLCA3 overexpression has a role in promoting intestinal mucus retention and goblet cell hypertrophy [73]. The increased staining of goblet cells treated with mCLCA3 would support the theory that it acts as a modifier of mucus secretion by inhibiting mucin degranulation. Importantly, these results confirm that mCLCA3 would be responsible for

the effects seen on goblet cells as it drives mucus production and/or is an inhibitor of mucus secretion.

IV. D. Summary

The *in vitro* study of mCLCA3 expression on HT29 cells provides a model for studying mucins and goblet cells in the colonic epithelium. Of the mucins that were analyzed, only MUC1 gene expression was significantly down-regulated by mCLCA3 in HT29 cells compared to other treatments. This could have a significant effect on mucus composition and rheology since MUC1 is expressed in all secretory epithelial cells. In addition to being a prospective marker for inflammatory airway disease, this could also potentially link mCLCA3/hCLCA1 as a tumor suppressor in the colon and other tissues. If regulation of MUC1 transcript levels by mCLCA3/hCLCA1 translates into the management or control of MUC1 protein synthesis, processing or function, it would certainly make it a viable avenue for future studies assessing its ability to control cell proliferation in carcinomas overexpressing MUC1.

Protein work showed that MUC3B protein levels of HT29-CaP and HT29trCLCA3 cultures differed despite showing no significant changes at the mRNA level. Since the MUC3B protein levels were not also significantly higher in HT29trCLCA3 cultures compared to the other controls, this increase cannot be directly attributed to mCLCA3 expression. The complex regulation of mucins is still not completely understood as a wide variety of transcription factors, translational factors and post-translational modifications exist that control mucus volume and its composition.

The effects of mCLCA3 expression on HT29 cells support its role as a modifier of goblet cell physiology. This directly implicates hCLCA1 to have a similar function on intestinal goblet cells, but this does not necessarily mean it would have the same effect in other tissues. In the lung, for example, mCLCA3/hCLCA1 regulation of mucin granule exocytosis from goblet cells could be superseded by other factors not present or active in the colon. Thus, a more physiologically relevant model would be required to study the *in vitro* regulation of goblet cell development in the lung, trachea, stomach and small intestine by mCLCA3/hCLCA1.

V. Future Directions

More work is still required to establish how mCLCA3/hCLCA1 has a role in CF and other mucous-based diseases. It has been shown here that mCLCA3 expression affects HT29 goblet cell morphometry. Further analysis of the effects of mCLCA3/hCLCA1 on mucus properties and goblet cells could be performed using exogenous protein overlays of fully-processed CLCA proteins onto cell cultures. This would simulate *in vivo* mature CLCA function, allowing for the analysis of the various mucins and goblet cell morphometry *in vitro*. As previously mentioned, in depth study of fully processed mucins and trefoil factor 3 on CLCA transfected epithelial layers will be facilitated as functional commercial antibodies become available.

How does mCLCA3/hCLCA1 regulate mucus secretion, mucin synthesis and processing? Despite evidence of CLCA regulation by various Th2 cytokines there is still no specific pathway that has been deciphered on the action of CLCA regulation. Structural domains of mCLCA3 are also thought to favour protein interaction but as of yet no binding partners have been found. Additional studies are required to reveal the regulation of mCLCA3/hCLCA1 expression and the subsequent function of these CLCA's in signal transduction. This would help to elucidate the effect of mCLCA3/hCLCA1 on goblet cell pathophysiology and makes them a potential therapeutic target for mucous-based lesions such as asthma, chronic obstructive pulmonary disease or cystic fibrosis.

VI. References

1. Quinton, P.M., *Chloride impermeability in cystic fibrosis*. Nature, 1983. **301**(5899): p. 421-2.
2. Bear, C.E., et al., *Purification and functional reconstitution of the cystic fibrosis transmembrane conductance regulator (CFTR)*. Cell, 1992. **68**(4): p. 809-18.
3. Zielenski, J., *Genotype and phenotype in cystic fibrosis*. Respiration, 2000. **67**(2): p. 117-33.
4. Riordan, J.R., et al., *Identification of the cystic fibrosis gene: cloning and characterization of complementary DNA*. Science, 1989. **245**(4922): p. 1066-73.
5. Gregory, R.J., et al., *Expression and characterization of the cystic fibrosis transmembrane conductance regulator*. Nature, 1990. **347**(6291): p. 382-6.
6. Anderson, M.P., et al., *Demonstration that CFTR is a chloride channel by alteration of its anion selectivity*. Science, 1991. **253**(5016): p. 202-5.
7. Anderson, M.P. and M.J. Welsh, *Calcium and cAMP activate different chloride channels in the apical membrane of normal and cystic fibrosis epithelia*. Proc Natl Acad Sci U S A, 1991. **88**(14): p. 6003-7.
8. Rowntree, R.K. and A. Harris, *The phenotypic consequences of CFTR mutations*. Ann Hum Genet, 2003. **67**(Pt 5): p. 471-85.
9. Zhang, Z.R., et al., *Determination of the functional unit of the cystic fibrosis transmembrane conductance regulator chloride channel. One polypeptide forms one pore*. J Biol Chem, 2005. **280**(1): p. 458-68.
10. Sheppard, D.N. and M.J. Welsh, *Structure and function of the CFTR chloride channel*. Physiol Rev, 1999. **79**(1 Suppl): p. S23-45.
11. Glozman, R., et al., *N-glycans are direct determinants of CFTR folding and stability in secretory and endocytic membrane traffic*. J Cell Biol, 2009. **184**(6): p. 847-62.
12. Kerem, B., et al., *Identification of the cystic fibrosis gene: genetic analysis*. Science, 1989. **245**(4922): p. 1073-80.
13. Rommens, J.M., et al., *Identification of the cystic fibrosis gene: chromosome walking and jumping*. Science, 1989. **245**(4922): p. 1059-65.
14. Gelman, M.S. and R.R. Kopito, *Cystic fibrosis: premature degradation of mutant proteins as a molecular disease mechanism*. Methods Mol Biol, 2003. **232**: p. 27-37.
15. Ward, C.L., S. Omura, and R.R. Kopito, *Degradation of CFTR by the ubiquitin-proteasome pathway*. Cell, 1995. **83**(1): p. 121-7.
16. Jensen, T.J., et al., *Multiple proteolytic systems, including the proteasome, contribute to CFTR processing*. Cell, 1995. **83**(1): p. 129-35.
17. Yang, Y., et al., *The common variant of cystic fibrosis transmembrane conductance regulator is recognized by hsp70 and degraded in a pre-Golgi nonlysosomal compartment*. Proc Natl Acad Sci U S A, 1993. **90**(20): p. 9480-4.
18. Wang, X., et al., *Hsp90 cochaperone Aha1 downregulation rescues misfolding of CFTR in cystic fibrosis*. Cell, 2006. **127**(4): p. 803-15.
19. Pind, S., J.R. Riordan, and D.B. Williams, *Participation of the endoplasmic reticulum chaperone calnexin (p88, IP90) in the biogenesis of the cystic fibrosis transmembrane conductance regulator*. J Biol Chem, 1994. **269**(17): p. 12784-8.

20. Meacham, G.C., et al., *The Hdj-2/Hsc70 chaperone pair facilitates early steps in CFTR biogenesis*. EMBO J, 1999. **18**(6): p. 1492-505.
21. Riordan, J.R., *CFTR function and prospects for therapy*. Annu Rev Biochem, 2008. **77**: p. 701-26.
22. Welsh, M.J. and A.E. Smith, *Cystic fibrosis*. Sci Am, 1995. **273**(6): p. 52-9.
23. Feranchak, A.P., *Hepatobiliary complications of cystic fibrosis*. Curr Gastroenterol Rep, 2004. **6**(3): p. 231-9.
24. Kaplan, E., et al., *Reproductive failure in males with cystic fibrosis*. N Engl J Med, 1968. **279**(2): p. 65-9.
25. Phillipson, G., *Cystic fibrosis and reproduction*. Reprod Fertil Dev, 1998. **10**(1): p. 113-9.
26. Pilewski, J.M. and R.A. Frizzell, *Role of CFTR in airway disease*. Physiol Rev, 1999. **79**(1 Suppl): p. S215-55.
27. Li, J.D., et al., *Transcriptional activation of mucin by Pseudomonas aeruginosa lipopolysaccharide in the pathogenesis of cystic fibrosis lung disease*. Proc Natl Acad Sci U S A, 1997. **94**(3): p. 967-72.
28. Ha, U., et al., *A novel role for IkappaB kinase (IKK) alpha and IKKbeta in ERK-dependent up-regulation of MUC5AC mucin transcription by Streptococcus pneumoniae*. J Immunol, 2007. **178**(3): p. 1736-47.
29. Kraft, M., et al., *Mycoplasma pneumoniae induces airway epithelial cell expression of MUC5AC in asthma*. Eur Respir J, 2008. **31**(1): p. 43-6.
30. Kreindler, J.L., *Cystic fibrosis: exploiting its genetic basis in the hunt for new therapies*. Pharmacol Ther. **125**(2): p. 219-29.
31. Sbarbati, A., et al., *Ultrastructural lesions in the small bowel of patients with cystic fibrosis*. Pediatr Res, 1998. **43**(2): p. 234-9.
32. Hodson, M.E., M.B. Mearns, and J.C. Batten, *Meconium ileus equivalent in adults with cystic fibrosis of pancreas: a report of six cases*. Br Med J, 1976. **2**(6039): p. 790-1.
33. Matsehe, J.W., V.L. Go, and E.P. DiMagno, *Meconium ileus equivalent complicating cystic fibrosis in postneonatal children and young adults. Report of 12 cases*. Gastroenterology, 1977. **72**(4 Pt 1): p. 732-6.
34. Dray, X., et al., *Distal intestinal obstruction syndrome in adults with cystic fibrosis*. Clin Gastroenterol Hepatol, 2004. **2**(6): p. 498-503.
35. Morton, A.M., *Symposium 6: Young people, artificial nutrition and transitional care. The nutritional challenges of the young adult with cystic fibrosis: transition*. Proc Nutr Soc, 2009. **68**(4): p. 430-40.
36. Rozmahel, R., et al., *Modulation of disease severity in cystic fibrosis transmembrane conductance regulator deficient mice by a secondary genetic factor*. Nat Genet, 1996. **12**(3): p. 280-7.
37. Zielenski, J., et al., *Detection of a cystic fibrosis modifier locus for meconium ileus on human chromosome 19q13*. Nat Genet, 1999. **22**(2): p. 128-9.
38. Heymans, H.S., *Gastrointestinal dysfunction and its effects on nutrition in CF*. Acta Paediatr Scand Suppl, 1989. **363**: p. 74-8; discussion 78-9.
39. Collaco, J.M. and G.R. Cutting, *Update on gene modifiers in cystic fibrosis*. Curr Opin Pulm Med, 2008. **14**(6): p. 559-66.

40. Gu, Y., et al., *Identification of IFRD1 as a modifier gene for cystic fibrosis lung disease*. *Nature*, 2009. **458**(7241): p. 1039-42.
41. Ritzka, M., et al., *The CLCA gene locus as a modulator of the gastrointestinal basic defect in cystic fibrosis*. *Hum Genet*, 2004. **115**(6): p. 483-91.
42. Tirkos S, et al., *Investigation of S100A8 as a modifier of lung disease in CF mice*. *Pediatr Pulmonol* 2001. **32**(S22): p. A299.
43. Brouillard, F., et al., *Blue native/SDS-PAGE analysis reveals reduced expression of the mCLCA3 protein in cystic fibrosis knock-out mice*. *Mol Cell Proteomics*, 2005. **4**(11): p. 1762-75.
44. Ran, S. and D.J. Benos, *Isolation and functional reconstitution of a 38-kDa chloride channel protein from bovine tracheal membranes*. *J Biol Chem*, 1991. **266**(8): p. 4782-8.
45. Zhu, D.Z., C.F. Cheng, and B.U. Pauli, *Mediation of lung metastasis of murine melanomas by a lung-specific endothelial cell adhesion molecule*. *Proc Natl Acad Sci U S A*, 1991. **88**(21): p. 9568-72.
46. Fuller, C.M., et al., *Ca(2+)-activated Cl(-) channels: a newly emerging anion transport family*. *Pflugers Arch*, 2001. **443 Suppl 1**: p. S107-10.
47. Cunningham, S.A., et al., *Cloning of an epithelial chloride channel from bovine trachea*. *J Biol Chem*, 1995. **270**(52): p. 31016-26.
48. Britton, F.C., et al., *Comparison of the properties of CLCA1 generated currents and I(Cl(Ca)) in murine portal vein smooth muscle cells*. *J Physiol*, 2002. **539**(Pt 1): p. 107-17.
49. Elble, R.C., et al., *Molecular and functional characterization of a murine calcium-activated chloride channel expressed in smooth muscle*. *J Biol Chem*, 2002. **277**(21): p. 18586-91.
50. Evans, S.R., W.B. Thoreson, and C.L. Beck, *Molecular and functional analyses of two new calcium-activated chloride channel family members from mouse eye and intestine*. *J Biol Chem*, 2004. **279**(40): p. 41792-800.
51. Gandhi, R., et al., *Molecular and functional characterization of a calcium-sensitive chloride channel from mouse lung*. *J Biol Chem*, 1998. **273**(48): p. 32096-101.
52. Gaspar, K.J., et al., *Cloning a chloride conductance mediator from the apical membrane of porcine ileal enterocytes*. *Physiol Genomics*, 2000. **3**(2): p. 101-11.
53. Gruber, A.D., et al., *Genomic cloning, molecular characterization, and functional analysis of human CLCA1, the first human member of the family of Ca2+-activated Cl- channel proteins*. *Genomics*, 1998. **54**(2): p. 200-14.
54. Romio, L., et al., *Characterization of a murine gene homologous to the bovine CaCC chloride channel*. *Gene*, 1999. **228**(1-2): p. 181-8.
55. Gruber, A.D., et al., *Molecular cloning and transmembrane structure of hCLCA2 from human lung, trachea, and mammary gland*. *Am J Physiol*, 1999. **276**(6 Pt 1): p. C1261-70.
56. Patel, A.C., T.J. Brett, and M.J. Holtzman, *The role of CLCA proteins in inflammatory airway disease*. *Annu Rev Physiol*, 2009. **71**: p. 425-49.
57. Agnel, M., T. Vermat, and J.M. Culouscou, *Identification of three novel members of the calcium-dependent chloride channel (CaCC) family predominantly expressed in the digestive tract and trachea*. *FEBS Lett*, 1999. **455**(3): p. 295-301.

58. Gruber, A.D. and B.U. Pauli, *Molecular cloning and biochemical characterization of a truncated, secreted member of the human family of Ca²⁺-activated Cl⁻ channels*. *Biochim Biophys Acta*, 1999. **1444**(3): p. 418-23.
59. Loewen, M.E. and G.W. Forsyth, *Structure and function of CLCA proteins*. *Physiol Rev*, 2005. **85**(3): p. 1061-92.
60. Mundhenk L, A.M., Elble RC, Pauli BU, Naim HY, Gruber AD., *Both cleavage products of the mCLCA3 protein are secreted soluble proteins*. *J Biol Chem.*, 2006. **281**(40): p. 30072-30080.
61. Komiya, T., Y. Tanigawa, and S. Hirohashi, *Cloning and identification of the gene gob-5, which is expressed in intestinal goblet cells in mice*. *Biochem Biophys Res Commun*, 1999. **255**(2): p. 347-51.
62. Leverkoehne, I. and A.D. Gruber, *Assignment of the murine calcium-activated chloride channel genes *Clca1* and *Clca3* (alias *gob-5*) to chromosome 3 band H2-H3 using somatic cell hybrids*. *Cytogenet Cell Genet*, 2000. **88**(3-4): p. 208-9.
63. Leverkoehne, I. and A.D. Gruber, *The murine mCLCA3 (alias *gob-5*) protein is located in the mucin granule membranes of intestinal, respiratory, and uterine goblet cells*. *J Histochem Cytochem*, 2002. **50**(6): p. 829-38.
64. Gibson A, L.A., Affleck K, Aitken AJ, Meldrum E, Thompson N., *hCLCA1 and mCLCA3 are secreted non-integral membrane proteins and therefore are not ion channels*. *J Biol Chem.*, 2005. **280**(29): p. 27205-27212.
65. Whittaker, C.A. and R.O. Hynes, *Distribution and evolution of von Willebrand/integrin A domains: widely dispersed domains with roles in cell adhesion and elsewhere*. *Mol Biol Cell*, 2002. **13**(10): p. 3369-87.
66. Tuckwell, D., *Evolution of von Willebrand factor A (VWA) domains*. *Biochem Soc Trans*, 1999. **27**(6): p. 835-40.
67. Bork, P. and R.F. Doolittle, *Proposed acquisition of an animal protein domain by bacteria*. *Proc Natl Acad Sci U S A*, 1992. **89**(19): p. 8990-4.
68. Nakanishi, A., et al., *Role of *gob-5* in mucus overproduction and airway hyperresponsiveness in asthma*. *Proc Natl Acad Sci U S A*, 2001. **98**(9): p. 5175-80.
69. Robichaud, A., et al., *Gob-5 is not essential for mucus overproduction in preclinical murine models of allergic asthma*. *Am J Respir Cell Mol Biol*, 2005. **33**(3): p. 303-14.
70. Sabo-Attwood, T., et al., *Gene expression profiles reveal increased *mClca3* (*Gob5*) expression and mucin production in a murine model of asbestos-induced fibrogenesis*. *Am J Pathol*, 2005. **167**(5): p. 1243-56.
71. Long, A.J., et al., *Gob-5 contributes to goblet cell hyperplasia and modulates pulmonary tissue inflammation*. *Am J Respir Cell Mol Biol*, 2006. **35**(3): p. 357-65.
72. Kent, G., et al., *Lung disease in mice with cystic fibrosis*. *J Clin Invest*, 1997. **100**(12): p. 3060-9.
73. Young FD, N.S., Choi C, Keet M, Kent G, Rozmahel RF., *Amelioration of cystic fibrosis intestinal mucous disease in mice by restoration of mCLCA3*. *Gastroenterology.*, 2007. **133**(6): p. 1928-1937.

74. Kuperman, D.A., et al., *Direct effects of interleukin-13 on epithelial cells cause airway hyperreactivity and mucus overproduction in asthma*. *Nat Med*, 2002. **8**(8): p. 885-9.
75. Zhou Y, D.Q., Louahed J, Dragwa C, Savio D, Huang M, Weiss C, Tomer Y, McLane MP, Nicolaides NC, Levitt RC., *Characterization of a calcium-activated chloride channel as a shared target of Th2 cytokine pathways and its potential involvement in asthma*. *Am J Respir Cell Mol Biol.*, 2001. **25**(4): p. 486-491.
76. Nakano, T., et al., *Niflumic acid suppresses interleukin-13-induced asthma phenotypes*. *Am J Respir Crit Care Med*, 2006. **173**(11): p. 1216-21.
77. Blanchard, C., et al., *IL-4 and IL-13 up-regulate intestinal trefoil factor expression: requirement for STAT6 and de novo protein synthesis*. *J Immunol*, 2004. **172**(6): p. 3775-83.
78. Tyner, J.W., et al., *Blocking airway mucous cell metaplasia by inhibiting EGFR antiapoptosis and IL-13 transdifferentiation signals*. *J Clin Invest*, 2006. **116**(2): p. 309-21.
79. Thai, P., et al., *Regulation of airway mucin gene expression*. *Annu Rev Physiol*, 2008. **70**: p. 405-29.
80. Rose, M.C. and J.A. Voynow, *Respiratory tract mucin genes and mucin glycoproteins in health and disease*. *Physiol Rev*, 2006. **86**(1): p. 245-78.
81. Deplancke, B. and H.R. Gaskins, *Microbial modulation of innate defense: goblet cells and the intestinal mucus layer*. *Am J Clin Nutr*, 2001. **73**(6): p. 1131S-1141S.
82. Specian, R.D. and M.G. Oliver, *Functional biology of intestinal goblet cells*. *Am J Physiol*, 1991. **260**(2 Pt 1): p. C183-93.
83. Davis, C.W. and B.F. Dickey, *Regulated airway goblet cell mucin secretion*. *Annu Rev Physiol*, 2008. **70**: p. 487-512.
84. Reader, J.R., et al., *Pathogenesis of mucous cell metaplasia in a murine asthma model*. *Am J Pathol*, 2003. **162**(6): p. 2069-78.
85. Evans, C.M., et al., *Mucin is produced by clara cells in the proximal airways of antigen-challenged mice*. *Am J Respir Cell Mol Biol*, 2004. **31**(4): p. 382-94.
86. Park, K.S., et al., *Transdifferentiation of ciliated cells during repair of the respiratory epithelium*. *Am J Respir Cell Mol Biol*, 2006. **34**(2): p. 151-7.
87. Specian, R.D. and M.R. Neutra, *Cytoskeleton of intestinal goblet cells in rabbit and monkey*. *The theca*. *Gastroenterology*, 1984. **87**(6): p. 1313-25.
88. Radwan, K.A., M.G. Oliver, and R.D. Specian, *Cytoarchitectural reorganization of rabbit colonic goblet cells during baseline secretion*. *Am J Anat*, 1990. **189**(4): p. 365-76.
89. Forstner, G., *Signal transduction, packaging and secretion of mucins*. *Annu Rev Physiol*, 1995. **57**: p. 585-605.
90. Li, Y., et al., *MARCKS protein is a key molecule regulating mucin secretion by human airway epithelial cells in vitro*. *J Biol Chem*, 2001. **276**(44): p. 40982-90.
91. Tarran, R., B. Button, and R.C. Boucher, *Regulation of normal and cystic fibrosis airway surface liquid volume by phasic shear stress*. *Annu Rev Physiol*, 2006. **68**: p. 543-61.
92. Voynow, J.A. and B.K. Rubin, *Mucins, mucus, and sputum*. *Chest*, 2009. **135**(2): p. 505-12.

93. Perez-Vilar, J., et al., *Mucin granule intraluminal organization in living mucous/goblet cells. Roles of protein post-translational modifications and secretion.* J Biol Chem, 2006. **281**(8): p. 4844-55.
94. Theodoropoulos, G. and K.L. Carraway, *Molecular signaling in the regulation of mucins.* J Cell Biochem, 2007. **102**(5): p. 1103-16.
95. Allen, A., *Structure of gastrointestinal mucus glycoproteins and the viscous and gel-forming properties of mucus.* Br Med Bull, 1978. **34**(1): p. 28-33.
96. Jensen, P.H., D. Kolarich, and N.H. Packer, *Mucin-type O-glycosylation--putting the pieces together.* FEBS J. **277**(1): p. 81-94.
97. Desseyn, J.L., D. Tetaert, and V. Gouyer, *Architecture of the large membrane-bound mucins.* Gene, 2008. **410**(2): p. 215-22.
98. Hattrup, C.L. and S.J. Gendler, *Structure and function of the cell surface (tethered) mucins.* Annu Rev Physiol, 2008. **70**: p. 431-57.
99. Chadee, K., et al., *Rat and human colonic mucins bind to and inhibit adherence lectin of Entamoeba histolytica.* J Clin Invest, 1987. **80**(5): p. 1245-54.
100. Kim, K.C., et al., *Pharmacology of airway goblet cell mucin release.* J Pharmacol Sci, 2003. **92**(4): p. 301-7.
101. Perez-Vilar, J., *Mucin granule intraluminal organization.* Am J Respir Cell Mol Biol, 2007. **36**(2): p. 183-90.
102. Verdugo, P., *Goblet cells secretion and mucogenesis.* Annu Rev Physiol, 1990. **52**: p. 157-76.
103. Bansil, R., E. Stanley, and J.T. LaMont, *Mucin biophysics.* Annu Rev Physiol, 1995. **57**: p. 635-57.
104. Ho, S.B., et al., *Cysteine-rich domains of muc3 intestinal mucin promote cell migration, inhibit apoptosis, and accelerate wound healing.* Gastroenterology, 2006. **131**(5): p. 1501-17.
105. Sheehan, J.K., M. Kesimer, and R. Pickles, *Innate immunity and mucus structure and function.* Novartis Found Symp, 2006. **279**: p. 155-66; discussion 167-9, 216-9.
106. Singh, P.K. and M.A. Hollingsworth, *Cell surface-associated mucins in signal transduction.* Trends Cell Biol, 2006. **16**(9): p. 467-76.
107. Gendler, S.J., *MUC1, the renaissance molecule.* J Mammary Gland Biol Neoplasia, 2001. **6**(3): p. 339-53.
108. Rossi, E.A., et al., *Sialomucin complex, a heterodimeric glycoprotein complex. Expression as a soluble, secretable form in lactating mammary gland and colon.* J Biol Chem, 1996. **271**(52): p. 33476-85.
109. Price-Schiavi, S.A., et al., *Sialomucin complex (rat Muc4) is regulated by transforming growth factor beta in mammary gland by a novel post-translational mechanism.* J Biol Chem, 2000. **275**(23): p. 17800-7.
110. Wright, N.A., et al., *Rolling in the clover: trefoil factor family (TFF)-domain peptides, cell migration and cancer.* FEBS Lett, 1997. **408**(2): p. 121-3.
111. Thim, L., *A new family of growth factor-like peptides. 'Trefoil' disulphide loop structures as a common feature in breast cancer associated peptide (pS2), pancreatic spasmodic polypeptide (PSP), and frog skin peptides (spasmodicins).* FEBS Lett, 1989. **250**(1): p. 85-90.

112. Thim, L. and F.E. May, *Structure of mammalian trefoil factors and functional insights*. Cell Mol Life Sci, 2005. **62**(24): p. 2956-73.
113. Carrasco, R., et al., *Trefoil factor family peptide 3 prevents the development and promotes healing of ischemia-reperfusion injury in weanling rats*. J Pediatr Surg, 2004. **39**(11): p. 1693-700.
114. Kinoshita, K., et al., *Distinct pathways of cell migration and antiapoptotic response to epithelial injury: structure-function analysis of human intestinal trefoil factor*. Mol Cell Biol, 2000. **20**(13): p. 4680-90.
115. Wong, W.M., R. Poulsom, and N.A. Wright, *Trefoil peptides*. Gut, 1999. **44**(6): p. 890-5.
116. Chinery, R. and R.J. Playford, *Combined intestinal trefoil factor and epidermal growth factor is prophylactic against indomethacin-induced gastric damage in the rat*. Clin Sci (Lond), 1995. **88**(4): p. 401-3.
117. FitzGerald, A.J., et al., *Synergistic effects of systemic trefoil factor family 1 (TFF1) peptide and epidermal growth factor in a rat model of colitis*. Peptides, 2004. **25**(5): p. 793-801.
118. Soriano-Izquierdo, A., et al., *Trefoil peptide TFF2 treatment reduces VCAM-1 expression and leukocyte recruitment in experimental intestinal inflammation*. J Leukoc Biol, 2004. **75**(2): p. 214-23.
119. Zhang, B.H., et al., *The therapeutic effect of recombinant human trefoil factor 3 on hypoxia-induced necrotizing enterocolitis in immature rat*. Regul Pept, 2003. **116**(1-3): p. 53-60.
120. Hoffmann, W., *Trefoil factors TFF (trefoil factor family) peptide-triggered signals promoting mucosal restitution*. Cell Mol Life Sci, 2005. **62**(24): p. 2932-8.
121. Taupin, D. and D.K. Podolsky, *Trefoil factors: initiators of mucosal healing*. Nat Rev Mol Cell Biol, 2003. **4**(9): p. 721-32.
122. Farrell, J.J., et al., *TFF2/SP-deficient mice show decreased gastric proliferation, increased acid secretion, and increased susceptibility to NSAID injury*. J Clin Invest, 2002. **109**(2): p. 193-204.
123. Mashimo, H., et al., *Impaired defense of intestinal mucosa in mice lacking intestinal trefoil factor*. Science, 1996. **274**(5285): p. 262-5.
124. Lefebvre, O., et al., *Gastric mucosa abnormalities and tumorigenesis in mice lacking the pS2 trefoil protein*. Science, 1996. **274**(5285): p. 259-62.
125. Jiang, G.X., et al., *IL-6/STAT3/TFF3 signaling regulates human biliary epithelial cell migration and wound healing in vitro*. Mol Biol Rep.
126. Hoffmann, W., *TFF (trefoil factor family) peptides and their potential roles for differentiation processes during airway remodeling*. Curr Med Chem, 2007. **14**(25): p. 2716-9.
127. Hoffmann, W., W. Jagla, and A. Wiede, *Molecular medicine of TFF-peptides: from gut to brain*. Histol Histopathol, 2001. **16**(1): p. 319-34.
128. Augeron, C. and C.L. Laboisse, *Emergence of permanently differentiated cell clones in a human colonic cancer cell line in culture after treatment with sodium butyrate*. Cancer Res, 1984. **44**(9): p. 3961-9.
129. Li, Y.Y., et al., *Macrophage-derived interleukin-6 up-regulates MUC1, but down-regulates MUC2 expression in the human colon cancer HT-29 cell line*. Cell Immunol, 2009. **256**(1-2): p. 19-26.

130. Comalada, M., et al., *The effects of short-chain fatty acids on colon epithelial proliferation and survival depend on the cellular phenotype*. J Cancer Res Clin Oncol, 2006. **132**(8): p. 487-97.
131. Loewen, M.E., et al., *pCLCA1 lacks inherent chloride channel activity in an epithelial colon carcinoma cell line*. Am J Physiol Gastrointest Liver Physiol, 2004. **287**(1): p. G33-41.
132. Anton, F., et al., *Overexpression of eCLCA1 in small airways of horses with recurrent airway obstruction*. J Histochem Cytochem, 2005. **53**(8): p. 1011-21.
133. Hauber, H.P., et al., *Expression of HCLCA1 in cystic fibrosis lungs is associated with mucus overproduction*. Eur Respir J, 2004. **23**(6): p. 846-50.
134. Yasuo, M., et al., *Relationship between calcium-activated chloride channel 1 and MUC5AC in goblet cell hyperplasia induced by interleukin-13 in human bronchial epithelial cells*. Respiration, 2006. **73**(3): p. 347-59.
135. Zhou, Y., et al., *A calcium-activated chloride channel blocker inhibits goblet cell metaplasia and mucus overproduction*. Novartis Found Symp, 2002. **248**: p. 150-65; discussion 165-70, 277-82.
136. Weaver, G.A., et al., *Cornstarch fermentation by the colonic microbial community yields more butyrate than does cabbage fiber fermentation; cornstarch fermentation rates correlate negatively with methanogenesis*. Am J Clin Nutr, 1992. **55**(1): p. 70-7.
137. Young, G.P., et al., *Wheat bran suppresses potato starch--potentiated colorectal tumorigenesis at the aberrant crypt stage in a rat model*. Gastroenterology, 1996. **110**(2): p. 508-14.
138. Whitlock, J.P., Jr., R. Augustine, and H. Schulman, *Calcium-dependent phosphorylation of histone H3 in butyrate-treated HeLa cells*. Nature, 1980. **287**(5777): p. 74-6.
139. Darzynkiewicz, Z., et al., *Effect of n-butyrate on cell cycle progression and in situ chromatin structure of L1210 cells*. Exp Cell Res, 1981. **136**(2): p. 279-93.
140. Roediger, W.E., *Role of anaerobic bacteria in the metabolic welfare of the colonic mucosa in man*. Gut, 1980. **21**(9): p. 793-8.
141. Scheppach, W., et al., *Effect of butyrate enemas on the colonic mucosa in distal ulcerative colitis*. Gastroenterology, 1992. **103**(1): p. 51-6.
142. Chantret, I., et al., *Epithelial polarity, villin expression, and enterocytic differentiation of cultured human colon carcinoma cells: a survey of twenty cell lines*. Cancer Res, 1988. **48**(7): p. 1936-42.
143. Kim, D.W., et al., *An efficient expression vector for stable expression in human liver cells*. Gene, 1993. **134**(2): p. 307-8.
144. Xiao, W., et al., *Adeno-associated virus as a vector for liver-directed gene therapy*. J Virol, 1998. **72**(12): p. 10222-6.
145. Teschendorf, C., et al., *Comparison of the EF-1 alpha and the CMV promoter for engineering stable tumor cell lines using recombinant adeno-associated virus*. Anticancer Res, 2002. **22**(6A): p. 3325-30.
146. Pauli, B.U., et al., *Molecular characteristics and functional diversity of CLCA family members*. Clin Exp Pharmacol Physiol, 2000. **27**(11): p. 901-5.

147. Boshell, M., et al., *The product of the human MUC1 gene when secreted by mouse cells transfected with the full-length cDNA lacks the cytoplasmic tail.* Biochem Biophys Res Commun, 1992. **185**(1): p. 1-8.
148. Thathiah, A., C.P. Blobel, and D.D. Carson, *Tumor necrosis factor-alpha converting enzyme/ADAM 17 mediates MUC1 shedding.* J Biol Chem, 2003. **278**(5): p. 3386-94.
149. Kufe, D., et al., *Differential reactivity of a novel monoclonal antibody (DF3) with human malignant versus benign breast tumors.* Hybridoma, 1984. **3**(3): p. 223-32.
150. Burchell, J.M., A. Mungul, and J. Taylor-Papadimitriou, *O-linked glycosylation in the mammary gland: changes that occur during malignancy.* J Mammary Gland Biol Neoplasia, 2001. **6**(3): p. 355-64.
151. Kingston, R.E., C.A. Chen, and H. Okayama, *Calcium phosphate transfection.* Curr Protoc Immunol, 2001. **Chapter 10**: p. Unit 10 13.
152. Patel AC, M.J., Kim EY, Alevy Y, Swanson S, Tucker J, Huang G, Agapov E, Phillips TE, Fuentes ME, Iglesias A, Aud D, Allard JD, Dabbagh K, Peltz G, Holtzman MJ., *Genetic segregation of airway disease traits despite redundancy of calcium-activated chloride channel family members.* Physiol Genomics., 2006. **25**(3): p. 505-513.
153. Tesfaiqzi, Y., *Regulation of mucous cell metaplasia in bronchial asthma.* Curr Mol Med, 2008. **8**(5): p. 408-15.